수의학박사학위논문

Preventive Effect of Molybdate on Non-Alcoholic Fatty Liver Disease

비알콜성 지방간 질환에 대한 몰리브덴산염의 예방적 효과

2019년 2월

서울대학교 대학원
수의병인생물학 및 예방수의학 (환경위생학) 전공
이 승 우

Preventive Effect of Molybdate on Non-Alcoholic Fatty Liver Disease

비알콜성 지방간 질환에 대한 몰리브덴산염의 예방적 효과

지도교수 류 덕 영

이 논문을 수의학박사학위논문으로 제출함

2018년 10월

서울대학교 대학원

수의병인생물학 및 예방수의학 (환경위생학) 전공

이 승 우

이승우의 박사학위논문을 인준함

2018년 12월

위 원 장 _____ 김 용 백 (인)

부위원장 _____ 류 덕 영 (인)

위 원 _____ 남 기 환 (인)

위 원 _____ 이 소 영 (인)

위 원 _____ 김 수 희 (인)

ABSTRACT

Preventive Effect of Molybdate on Non-Alcoholic Fatty Liver Disease

Seungwoo Lee
Laboratory of Veterinary Environmental Health
Veterinary Pathobiology and Preventive Medicine
Department of Veterinary Medicine
The Graduate School
Seoul National University

Non-alcoholic fatty liver disease (NAFLD) is categorized into non-alcoholic fatty liver (NAFL) and non-alcoholic steatohepatitis (NASH) and has emerged as a common public health problem that can progress to end-stage liver disease, such as cirrhosis and hepatocellular carcinoma (HCC). However, the underlying mechanisms of NAFLD pathogenesis are not fully understood and there are no medications approved by the Federal Drug Administration for the treatment of NAFLD.

Hepatic steatosis, characterized with excessive hepatic

lipid accumulation, is the hallmark pathological finding in NAFLD and oxidative stress is a major pathologic contributor to development of NAFLD. The endoplasmic reticulum (ER) stress caused by accumulation of unfolded proteins in the ER may play an important role in the progression and development of NAFLD. Autophagy plays a major role in cellular homeostasis and impaired autophagy may contribute to the pathogenesis of NAFLD. Autophagy and apoptosis are interconnected stress response pathways.

In the present study, expression of proteins associated with ER stress, autophagy and apoptosis was analyzed in human NAFL and NASH tissues to elucidate the roles of those proteins in pathogenesis of NAFLD. Levels of some ER stress transducing transcription factors, such as cleaved activating transcription factor 6 (ATF6), spliced X-box binding protein 1 (XBP1s) and CCAAT/enhancer binding protein (C/EBP) homologous protein (CHOP), were higher in NASH than in the normal tissues. However, the expression of a majority of the ER chaperones and foldases analyzed, including glucose-regulated protein 78 (GRP78) and protein disulfide isomerase (PDI), was lower in NASH than in the normal tissues. Levels of apoptosis markers, such as cleaved poly (ADP-ribose) polymerase (PARP), were also lower in NASH

tissues, in which expression of some B-cell lymphoma-2 (Bcl-2) family proteins was up- or down-regulated compared to the normal tissues. The level of the autophagy substrate p62 was not different in NASH and normal tissues, although some autophagy regulators, such as autophagy protein 16L1 (ATG16L1) and microtubule-associated proteins 1A/1B light chain 3-II (LC3-II), were up-regulated in the NASH tissues compared to the normal tissues. Levels of most of the proteins analyzed in NAFL tissues were either similar to those in one of the other two types, NASH and normal, or were somewhere in between. These findings suggest that regulation of certain important tissues processes involved in the unfolded protein response (UPR) and apoptosis were broadly compromised in human NAFLD tissues.

A previous study reported that treatment with molybdate reduces hepatic levels of lipids in diabetic rats. Potential activities of molybdate as an antioxidant have also been demonstrated in various animal models. Accordingly, I evaluated the effects of sodium molybdate dihydrate (SM) on hepatic steatosis and associated disturbances in a widely used mouse model of the metabolic disease. Male C57BL/6 mice at 10 weeks of age were fed a methionine- and choline-deficient diet (MCD) and bottled water containing SM for four weeks. The

SM treatment markedly attenuated MCD-induced accumulation of lipids, mainly triglycerides, in the liver. Lipid catabolic autophagic pathways were activated by SM in the MCD-fed mouse livers, as evidenced by increased formation of LC3-II together with decreased levels of the autophagic substrate p62. MCD-induced oxidative damage, such as lipid and protein oxidation, was also alleviated by SM in the liver. However, the SM treatment did not affect the expression of ER stress-related proteins in the MCD-fed mouse livers. The level of MCD-induced hepatocellular damage was not also affected by SM. These findings suggest that molybdate effectively prevents MCD-induced lipid accumulation without causing adverse effects in the mouse liver, and that the lipid catabolic processes may involve the activation of autophagy.

Taken together, the present study may provide an insight into the pathogenesis of human NAFLD and suggests a beneficial effect of molybdate in the treatment and prevention of NAFLD.

Keywords: NAFLD, molybdate, ER stress, oxidative stress, autophagy, apoptosis
Student Number: 2012-21546

LIST OF CONTENTS

LIST OF TABLES

LIST OF FIGURES

CHAPTER I. DYSREGULATED EXPRESSION OF PROTEINS ASSOCIATED WITH ENDOPLASMIC RETICULUM STRESS, AUTOPHAGY AND APOPTOSIS IN TISSUES FROM HUMAN NON-ALCOHOLIC FATTY LIVER DISEASE

LIST OF ABBREVIATIONS

Alms1	alstrom syndrome protein 1
ALP	alkaline phosphatase
ALT	alanine aminotransferase
AOX	aldehyde oxidase
AST	aspartate transaminase
ATF6	activating transcription factor 6
ATG3	autophagy protein 3
ATG5	autophagy protein 5
ATG7	autophagy protein 7
ATG12	autophagy protein 12
ATG16L1	autophagy protein 16L1
Bak	bcl-2 homologous antagonist/killer
Bcl-2	b-cell lymphoma-2
Bim	bcl-2-like protein 11
CDF	choline-deficient high-fat diet
CHO	cholesterol
CHOP	CCAAT/enhancer binding protein (C/EBP) homologous protein
db/db	$Lepr^{db}/Lepr^{db}$
DTT	dithiothreitol
ER	endoplasmic reticulum
Ero1	ER oxireductin 1
ERp44	ER protein 44

ERp72	ER protein 72
FFA	free fatty acid
foz/foz	alms1 mutant
GAPDH	glyceraldehyde-3-phosphate dehydrogenase
GGT	gamma-glutamyl transferase
GRP78	glucose-regulated protein 78
GRP94	glucose-regulated protein 94
H&E	hematoxylin and eosin
HCC	hepatocellular carcinoma
HFD	high-fat diet
IgG	immunoglobulin G
IHC	immunohistochemistry
IRE1	inositol requiring enzyme 1
LC3	microtubule-associated proteins 1A/1B light chain 3
Lep	leptin
Lepr	leptin receptor
MCD	methionine- and choline-deficient diet
Mcl-1	myeloid cell leukemia-1
MDA	malondialdehyde
Mo	molybdenum
MoCo	molybdenum cofactor
MOCS	molybdenum cofactor synthesis
NAFL	non-alcoholic fatty liver
NAFLD	non-alcoholic fatty liver disease
NASH	non-alcoholic steatohepatitis

ob/ob	*Lep*^{ob}/*Lep*^{ob}
PARP	poly (ADP-ribose) polymerase
PDI	protein disulfide isomerase
PLIN2	perilipin 2
PERK	protein kinase RNA-like ER kinase
PMSF	phenylmethylsulfonyl fluoride
PPAR	proliferator-activated receptor
ROS	reactive oxygen species
SM	sodium molybdate dihydrate
SOD	superoxide dismutase
SOD1	cytoplasmic Cu/ZnSOD
SOD2	mitochondrial MnSOD
SOD3	extracellular Cu/ZnSOD
SUOX	sulfite oxidase
TG	triglyceride
UPR	unfolded protein response
VDAC1	voltage-dependent anion-selective channel 1
XBP1s	spliced x-box binding protein 1
XDH	xanthine oxidase/dehydrogenase

LITERATURE REVIEW

1. Non-alcoholic Fatty Liver Disease

1.1. Introduction

Non-alcoholic fatty liver disease (NAFLD) is defined as hepatic fat accumulation exceeding 5−10% of liver weight in the absence of other causes of steatosis, such as alcohol abuse and some hepatic viral infections. The disease was first reported by Ludwig et al. (1980) who described histological features similar to alcoholic hepatitis. NAFLD has a spectrum ranging from non-alcoholic fatty liver (NAFL), which is usually non-progressive and benign, to non-alcoholic steatohepatitis (NASH). NAFL is characterized by steatosis with no or minor inflammation, while NASH is characterized by the presence of steatosis with inflammation and fibrosis (Marrero et al., 2002; Farrell and Larter, 2006; Chalasani et al., 2012).

Day and James (1998) proposed the 'two-hit' hypothesis for the development of NAFLD. According to this hypothesis, the 'first hit' involves an imbalance in lipid metabolism that leads to NAFL, whereas the 'second hit' involves oxidative stress and mitochondrial dysfunction, which ultimately cause liver damage. The 'two-hit' hypothesis has subsequently been revised to 'multiple parallel hit' hypothesis (Tilg and Moschen,

2010). The hypothesis proposed that NASH is the result of numerous conditions acting in parallel, including abnormal lipid metabolism, lipotoxicity, altered production of cytokines and adipokines, oxidative stress, endoplasmic reticulum (ER) stress, mitochondrial dysfunction, genetic predisposition and gut dysbiosis.

1.2. Prevalence

NAFLD is currently the most common cause of chronic liver disease in western countries. About 20% all adults have NAFL and 2−3% of adults have NASH (Neuschwander-Tetri, 2005). 5−20% of patients with NAFL can progress to NASH (Weiß et al., 2014). Approximately 20% of patients with NASH are at risk for developing cirrhosis (Neuschwander-Tetri, 2005). In addition, 4−29% of patients with NASH can progress to hepatocellular carcinoma (HCC) (Clarke et al., 2014).

The prevalence of NAFLD is increasing worldwide due to lifestyle and dietary factors (Farrell and Larter, 2006). Global prevalence of NAFLD is 25% with highest prevalence in the Middle East (32%) and South America (31%) and lowest in Africa (14%) (Younossi et al., 2016). It has been shown that 70−80% of subjects with obesity and 50−80% of patients with type 2 diabetes have evidence of NAFLD. NAFLD was also

diagnosed in 32% of subjects with dyslipidemia (Fan et al., 2005; Targher et al., 2007; Williams et al., 2011; Williamson et al., 2011).

NAFLD can affect any age range, but its prevalence increases over time and is highest among older adults (Karnikowski et al., 2007). Frith et al. (2009) also found that older patients with NASH tend to have more fibrosis of the liver than young patients. Most studies have shown that male gender is associated with an increased prevalence of NAFLD (Shen et al., 2003; Weston et al., 2005; Arun et al., 2006; Chen et al., 2006; Zelber-Sagi et al., 2006; Lazo et al., 2013; Xiao et al., 2014). However, the role of gender in development of NAFLD is still controversial, as some studies have reported differing conclusions (Eguchi et al., 2012; Wong et al., 2012; Younossi et al., 2012).

1.3. Diagnosis

Liver biopsy is the gold standard for the diagnosis of NAFLD. Some diagnostic systems were developed for discrimination between NAFL and NASH (Dyson et al., 2014). The NAFLD activity score is the most widely used histological grading and staging system for NAFLD (Kleiner et al., 2005). The NAS is defined as the unweighted sum of the scores for

steatosis (0−3), lobular inflammation (0−3), and ballooning (0−2). Cases with scores < 3 are diagnosed as not NASH, and scores ≥ 5 are diagnosed as NASH.

The liver biopsy is not only invasive but also has medical problems and limitations. Accordingly, non-invasive techniques for diagnosis of NAFLD are increasingly used. Blood test is one of the most widely used non-invasive test for diagnosis of NAFLD. The following hepatic enzymes are commonly used for blood tests (Wilson and Chalasani, 2007).

Alanine/aspartate aminotransferase (ALT/AST)

ALT and AST are enzymes involved in the metabolism of amino acids. ALT is limited primarily to liver, whereas AST is found in various tissues, including heart, muscle, kidney and leukocyte; thus, ALT is a more sensitive and specific marker of hepatocellular damage than AST (Giannini et al., 2005). Elevated serum levels of AST and ALT are often found in NAFLD patients. The ratio of AST/ALT usually is less than 1 in patients with NAFLD, and tends to increase with the development of cirrhosis (Angulo et al., 1999).

Alkaline phosphatase (ALP)

ALP is a hydrolase enzyme that removes phosphate

groups from many types of molecules, such as nucleotides and proteins. ALP is made mostly in liver and bone, with some produced in intestine and kidney (Oh et al., 2015). Higher serum level of ALP is considered as a fibrosis-related marker in patients with NASH (Yoshida, 2011).

Gamma-glutamyl transferase (GGT)

GGT is a membrane-bound glycoprotein widely distributed in various tissues, including liver, kidney and pancreas (Mancinelli and Ceccanti, 2009). Seurm level of GGT is frequently elevated in patients with NAFLD (Haring et al., 2009). Increased serum level of GGT has been shown to be associated with advanced fibrosis in NAFLD patients (Tahan et al., 2008).

1.4. Molecular pathways in NAFLD

It was reported that a number of molecular pathways, such as oxidative stress, ER stress, autophagy, apoptosis and inflammation, have been implicated in the pathogenesis and progression of NAFLD. However, data regarding the role of these molecular pathways in human NAFLD are still limited.

Oxidative stress

Oxidative stress induced by the imbalance between antioxidants and reactive oxygen species (ROS) causes cellular damage to DNA, proteins and lipids. Levels of oxidative damage, such as lipid peroxidation and DNA fragmentation, tend to increase in the livers of patients with NAFLD (Seki et al., 2002; Malaguarnera et al., 2005; Fujita et al., 2009; Hardwick et al., 2010). In addition, decreased antioxidant activity is observed in human NAFLD liver (Krautbauer et al., 2013).

ER stress

ER stress is defined the accumulation of unfolded proteins in the ER. The ER stress disrupts lipid metabolism and induces hepatic lipotoxicity (Han and Kaufman, 2016). Induction of ER stress was observed by enhanced expression of ER stress markers, such as CCAAT/enhancer binding protein (C/EBP) homologous protein (CHOP) and spliced X-box binding protein 1 (XBP1s), in the livers of patients with NAFLD (González-Rodríguez et al., 2014; Lake et al., 2014).

Autophagy

Autophagy is an intracellular pathway responsible for the turnover of unwanted proteins or organelles (Mizushima and

Levine, 2010). Autophagy can also regulate intracellular lipid levels by removing lipid droplets through a process known as lipophagy (Singh et al., 2009). The impairment of autophagy was observed in the livers of patients with NAFLD (Fukuo et al., 2014; González-Rodríguez et al., 2014; Tu et al., 2014).

Apoptosis

Apoptosis is nature's pre-programmed form of cell death which is characterized by organized cellular fragmentation. Apoptosis can be triggered by two alternative pathways, such as the extrinsic death receptor-mediated pathway or the intrinsic intracellular organelle-based pathway (Green and Reed, 1998). An increase in hepatocyte cell death by apoptosis is typically present in patients with NASH, but is absent in those with NAFL (Feldstein et al., 2003).

Inflammation

Inflammation is a physiological response to tissue injury or infection that leads to secretion of various inflammatory mediators, such as cytokines and chemokines. Chronic liver inflammation is an important contributing factor to the pathogenesis of NASH and the key predictor of histological progression of fibrosis (Schuster et al., 2018).

1.5. Pharmacological therapeutics of NAFLD

Dietary changes and lifestyle modifications are considered as the first-line therapy for patients with NAFLD. However, there is still a need for pharmacological therapeutics to improve the disease progression. Many therapeutic agents have been tested for the treatment of NAFLD (Table 1). Pharmacological treatments focus on reduction of disturbances associated with NAFLD.

Table 1. Pharmacologic agents and their effect on human NAFLD.

	Dose of treatment	ALT or AST	NAFL	NASH	Fibrosis
Elafibranor	120 mg/day	↓	↓	↓	↓
Pentoxifylline	400 mg three times/day	↓	↓	↓	↓
Obeticholic acid	25 mg/day	↓	↓	↓	↓
Pioglitazone	45 mg/day	↓	↓	↓	↔
Liraglutide	1.8 mg/day	↓	↓	↓	↔
Vitamin E	400−800 IU/day	↓	↓	↓	N.S
Metformin	2000 mg/day	↓	↓	↔	↔
Vildagliptin	50 mg two times/day	↓	↓	N.S	N.S
Exenatide	2.0 g/day	↓	↓	N.S	N.S

ALT, alanine aminotransferase; AST, aspartate aminotransferase; NAFL, non-alcoholic fatty liver; NASH, non-alcoholic steatohepatitis; N.S, not shown.

Elafibranor/Pentoxifylline/Obeticholic acid

Elafibranor is a proliferator-activated receptor (PPAR)-α/δ agonist that increases lipid oxidation and inhibits macrophage activation. Pentoxifylline, a non-selective phosphodiesterase inhibitor, has anti-inflammatory effects and decreases oxidative stress. Obeticholic acid is a potent activator of the farnesoid X nuclear receptor. These three agents improve hepatotoxicity, NAFL, NASH and hepatic fibrosis in humans (Zein et al., 2011; Neuschwander-Tetri et al., 2015; Ratziu et al., 2016).

Pioglitazone/Liraglutide

Pioglitazone is a peroxisome PPAR-γ agonist that has also been shown to improve hepatotoxicity, NAFL and NASH in humans (Belfort et al., 2006). Liraglutide is a glucagon-like peptide-1 agonist and is used in the treatment of type 2 diabetes and obesity. The efficacy of liraglutide was also reported in NAFL and NASH patients (Armstrong et al., 2016).

Vitamin E

Vitamin E is an antioxidant believed to reduce hepatocyte oxidative stress in patients with NASH (Rinella, 2015). It improves hepatotoxicity, NAFL and NASH but has not

yet been shown to improve hepatic fibrosis in humans (Lavine et al., 2011; Sato et al., 2015).

Metformin

Metformin is considered first-line therapy for the management in type 2 diabetes. Metformin was studied in several clinical trials, and it exhibited beneficial effects on NAFL and hepatotoxicity (Bugianesi et al., 2005; Loomba et al., 2009). However, it does not improve NASH and fibrosis.

Vildagliptin/Exenatide

Vildagliptin, a dipeptidyl peptidase-4 inhibitoris, is used to treat type 2 diabetes. Exenatide, a synthetic analog of exendin-4, is also an anti-diabetic agent. These two agents have potential roles in the treatment of NAFL (Fan et al., 2013; Hussain et al., 2016).

1.6. Animal models of NAFLD

Animal models of NAFLD provide critical guidance for understanding its pathogenesis and for identification of new therapeutic targets. An ideal animal model of NAFLD should incorporate the following criteria: (1) the pathological patterns and histological alterations found in the different stages of

human NAFLD and (2) the general physiological alterations associated with the development of human NAFLD (Tilg and Moschen, 2010). Numerous animal models of NAFLD have been reported to date, and are generally classified into genetic and dietary models (Table 2).

Table 2. Characteristics of commonly used animal models of NAFLD.

		NAFL	NASH	Fibrosis	HCC	Obesity	Insulin resistance
Genetic models	db/db	Yes	No	No	No	Yes	Yes
	ob/ob	Yes	No	No	No	Yes	Yes
	foz/foz	Yes	Yes	Yes	No	Yes	Yes
Dietary models	HFD	Yes	Yes	Yes	No	Yes	Yes
	MCD	Yes	Yes	Yes	No	No	No
	CDF	Yes	Yes	Yes	Yes	Yes	No

NAFL, non-alcoholic fatty liver; NASH, non-alcoholic steatohepatitis; HCC, hepatocellular carcinoma; db/db, $Lepr^{db}/Lepr^{db}$; ob/ob, Lep^{ob}/Lep^{ob}; foz/foz, a*lms1* mutant; HFD, high-fat diet; MCD, methionine- and choline-deficient diet; CDF, choline-deficient high-fat diet.

$Lepr^{db}/Lepr^{db}$ (db/db)

Type 2 diabetic db/db mice possess a point mutation in the leptin receptor (*Lepr*) gene and, therefore, show normal or

elevated levels of leptin but are resistant to the effects of leptin. These mice develop NAFL, and are obese, diabetic and insulin resistant (Trak-Smayra et al., 2011). However, the db/db mice do not spontaneously develop NASH or fibrosis.

Lep^{ob}/*Lep*^{ob} (ob/ob)

Obese ob/ob mice possess a spontaneous mutation in the leptin (*Lep*) gene, which renders them leptin-deficient. Similar to db/db mice, these mice are grossly overweight and resistant to insulin, and develop spontaneous NAFL but not NASH (Trak-Smayra et al., 2011). The ob/ob mice are resistant to fibrosis (Leclercq et al., 2002).

Alms1 mutant (foz/foz)

Appetite-defective foz/foz mice have a mutated alstrom syndrome protein 1 (*Alms1*) gene, which encodes a protein found in the basal body of the primary cilium. The foz/foz mice spontaneously develop obesity, severe insulin resistance, and diabetes (Arsov et al., 2006). These mice develop NAFL, NASH and fibrosis (Mridha et al., 2017).

High-fat diet (HFD)

HFD (45 or 60 kcal% fat) feeding is commonly used in

mice models to induce NAFLD. Mice fed HFD exhibit obesity, insulin resistance and hyperlipidemia. These mice develop NAFL after 1−12 weeks and NASH after 24 weeks (Kim et al., 2014; Rao et al., 2016). Hepatic fibrosis is induced in mice after 36−50 weeks of HFD feeding (Kim et al., 2014).

Methionine- and choline-deficient diet (MCD)

MCD contains 40% sucrose and 10% fat, but is deficient in methionine and choline. MCD is a commonly used mice models of NAFLD, especially NASH, and is known to cause weight loss. NAFL and NASH develop much more quickly and severely than in mice fed HFD. NASH occurs at 4 weeks, and fibrosis is observed by 8−10 weeks in the liver of mice fed MCD (Ip et al., 2004; Machado et al., 2015). These mice does not exhibit insulin resistance (Rinella and Green, 2004).

Choline-deficient high-fat diet (CDF)

CDF is choline-deficient diet containing 60 kcal% of fat and 0.1% of methionine. CDF-fed mice develop NAFL, NASH and hepatic fibrosis more rapidly and severely than the conventional models (Matsumoto et al., 2013). In addition, CDF feeding induced development of hepatocellular adenoma and HCC at 36 weeks (Ikawa-Yoshida et al., 2017).

2. Molybdenum

2.1. Introduction

Molybdenum (Mo) is the 42nd element of the periodic table of the chemical elements. It was discovered in 1778 by Scheele and isolated in 1782 by Hjelm (Jarrell et al., 1980). Mo has several oxidation states from II to VI, the most common and stable of which are IV and VI (Khademi et al., 2009).

Mo is bioavailable as molybdate (MoO_4^{2-}) and is an essential trace element for most living beings from bacteria to animals (Bortels, 1930). Mo needs to be coordinated to a unique pterin, thus forming a prosthetic group named molybdenum cofactor (MoCo) at the catalytic sites of Mo-containing enzymes (Mendel and Kruse, 2012; Murray et al., 2014). Organisms meet Mo requirements using specific molybdate transporters. Bacterial molybdate transporters are well known and widely described. Most of these transporters belong to the ATP-binding cassette family (Grunden and Shanmugam, 1997). Proteins associated with the bacterial molybdate transport system are not encoded by eukaryotic genomes. For examples, molybdate transporter type 1 proteins are present in bacteria, algae, fungi, and plants but not in animal genomes

(Tejada-Jiménez et al., 2007). The molybdate transporters are still not well studied in animals and humans. Recently, human molybdate transporter type 2, a member of the family of sulfate transporters, had been reported to exhibit molybdate uptake activity in a yeast over-expression system (Tejada-Jiménez et al., 2011). The molybdate transporter type 2 is present on the plasma membrane of human cells.

Trace amounts of Mo are found in a wide variety of foods, and human exposure to Mo may occur in various different ways, such as diet, drinking water, or inhalation from occupational exposure (Murray et al., 2014). Mo is absorbed from gastrointestinal tract and distributed to liver in human (Novotny and Turnlund, 2007). The absorbed Mo is excreted mainly in the urine with small amounts excreted in the bile (Turnlund et al., 1995). The highest concentrations of Mo (more than 1 mg/kg of dry weight) are found in the liver, kidney and bone (Johnson, 1997). The concentrations of Mo are between 140 and 200 μg/kg dry weight in other tissues.

2.2. Mo-containing enzymes

Mo-containing enzymes, including aldehyde oxidase (AOX), xanthine oxidase/dehydrogenase (XDH) and sulfite oxidase (SUOX), have been identified in mammals (Mendel and

Kruse, 2012). The Mo-containing enzymes are important for diverse metabolic processes in mammals (Kisker et al., 1998). AOX is a cytosolic enzyme responsible for the metabolism of drugs and xenobiotics. AOX catalyzes the oxidative hydroxylation of substrates including several aliphatic and aromatic aldehydes, and nitrogen-containing heterocyclic fragments (Hutzler et al., 2012). XDH is a ubiquitous enzyme involved in purine metabolism which catalyzes the oxidation of hypoxanthine and xanthine to uric acid. XDH functions as a key regulator of inflammatory cascades (Ives et al., 2015). Activation of XDH can produce abundant reactive oxygen species (Fransen et al., 2012). SUOX is an essential enzyme in the pathway of the oxidative degradation of sulfite to sulfate protecting cells from sulfite toxicity (Cohen et al., 1973).

2.3. MoCo deficiency

MoCo deficiency is a rare and lethal autosomal-recessive disorder, for which until now no effective therapy is available. The disorder is classified in three types A, B, anc C (Hänzelmann et al., 2002). Type A is commonest, with mutations identified in molybdenum cofactor synthesis (*MOCS)* 1 gene (Reiss et al., 2005). Type B is caused by mutations in *MOCS2* gene. Type C is caused by mutations in *Gephyrin*

gene. MoCo deficiency in humans results in the simultaneous loss of all Mo-containing enzyme activities. Patients with MoCo deficiency present with neonatal seizures, feeding difficulties, severe developmental delay, brain atrophy and early childhood death (Jakubiczka-Smorag et al., 2016). Similar to humans, *Mocs1*-deficient mice died between days 1 and 11 after birth (Lee et al., 2002). In addition, no active MoCo was detectable, and consequently all Mo enzyme activities were absent.

2.4. Mo deficiency

Mo deficiency is rare in humans and animals (Rajagopalan, 1988) and may be caused by MoCo deficiency (Mendel, 2007). Long-term Mo deficiency has been observed in some humans and linked to an increased risk of esophageal cancer (Nouri et al., 2008; Ray et al., 2012). Mo deficiency also may be an important factor in the causation of gastric disease. Zhou et al. (1990) found that Mo level in the mucosa of patients with gastritis or gastric ulcer was lower than that of normal people, and that its level in mucosa of gastric cancer patients was also decreased. Mo deficiency has recently been demonstrated as the predisposing factor for some animal syndromes, such as amyotrophic lateral sclerosis and motor neuron disease (Bourke, 2016). In animals, diets low in Mo

resulted in detrimental effects associated with reproduction (Anke et al., 1990). Goats had poor conception rates and fetal survival. Chicks suffered high embryonic mortality and abnormal growth and development. It is possible to produce a deficiency of Mo in rats by the supplement of tungsten (Yoshida et al., 2015).

2.5. Mo-induced toxicity

The Food and Nutrition Board of the National Research Council states that a safe adequate intake of Mo is 75 to 350 μg/day for adults and 25 to 75 μg/day for children aged 1−6 years (Beers and Berkow, 1999). There are very few data on toxicity of Mo and its lethal doses in humans. A human study has shown that high dietary levels of Mo (300−800 μg Mo/day) can develop acute psychosis consisting of visual or auditory hallucinations (Momcilović, 1999). The Mo-poisoned patient was diagnosed toxic encephalopathy with executive deficiencies, learning disability, major depression, and post-traumatic stress disorder after one year. Gout-like symptoms have been reported among workers exposed to Mo (Walravens et al., 1979), as well as among the general population living in an area with high Mo contents in soil and vegetables (Kovalskiy et al., 1961). In addition, a high intake of

Mo could possibly cause decreased bone growth and bone mineral density (Lewis et al., 2016). Some human studies showed a significant relationship between increased Mo in the blood and decreased levels of circulating testosterone, as well as decreased sperm count and quality (Meeker et al., 2008, 2010).

Most of the toxicity data pertaining to Mo is in animals. There is considerable variability in the toxicity of Mo, depending on the chemical form and the animal species. Soluble Mo compounds, such as sodium molybdate dihydrate (SM), are more toxic than insoluble (Vyskocil and Viau, 1999). The symptoms of Mo toxicity, known as molybdenosis, are reported to resemble those of copper deficiency (Deosthale and Gopalan, 1974). The molybdenosis is characterised by growth depression, reproductive failure, diarrhea and anemia in animals (Walravens et al., 1979). In cattle and sheep, high dietary levels of Mo have been linked to reduced growth, kidney failure, infertility and diarrhea (Lamand et al., 1980; Raisbeck et al., 2006). Toxicity studies in rats have suggested that oral administration of SM at daily dose levels of 30 and 50 mg/kg/day can induce testicular damage (Pandey and Singh, 2002). Recently, the lowest-observed-adverse-effect level and no-observed-adverse-effect level for Mo in rats were

determined to be 60 and 17 mg Mo/kg body weight/day, respectively (Murray et al., 2014).

2.6. Beneficial effects of Mo

Mo can help reduce the levels of copper in the body. This process is being investigated as a treatment for some chronic diseases. Tetrathiomolybdate has the ability to reduce copper levels and is being researched as a potential treatment for Wilson's disease, cancer and multiple sclerosis (Redman et al., 2003; Brewer et al., 2009; Gartner et al., 2009).

Pre-treatment with molybdate protects against the acute toxicity of heavy metals such as lead, mercury and cadmium (Yamane and Koizumi, 1982; Yamane et al., 1990; Flora et al., 1993). Molybdate may also prevent certain forms of cancer induced by N-nitroso compounds such as forestomach, oesophageal and mammary gland cancer in rats (Luo et al., 1983; Wei et al., 1985). The findings of recent researches have revealed that molybdate has an insulin-mimicry activity and improves immune dysfunction associated with diabetes in rats (Panneerselvam and Govindasamy, 2003). Normalisation of glucose and lipid levels in streptozotocin-diabetic rats by orally administered molybdate was observed (Lord et al., 1999; Thompson et al., 2004). In addition, molybdate prevents lipid

oxidation and improves antioxidant systems during diabetes mellitus (Panneerselvam and Govindasamy, 2004). The beneficial effects of molybdate treatment on post ischemic cardiac function of diabetic rats was also observed (Jelikic-Stankova et al., 2007). Molybdate also attenuates chemically induced hepatic steatosis in rats (Eidi et al., 2011). More recently, Ale-Ebrahim et al. (2015) reported the hepatoprotective and antifibrotic effects of molybdate in the cholestatic liver.

CHAPTER I

DYSREGULATED EXPRESSION OF PROTEINS ASSOCIATED WITH ENDOPLASMIC RETICULUM STRESS, AUTOPHAGY AND APOPTOSIS IN TISSUES FROM HUMAN NON-ALCOHOLIC FATTY LIVER DISEASE

1. Introduction

NAFLD is a pathological condition histologically categorized into NAFL and NASH (Chalasani et al., 2012). NAFLD can progress to cirrhosis and end-stage liver diseases such as HCC (Ascha et al., 2010; Younossi et al., 2015).

Accumulation of unfolded proteins in the ER causes ER stress, which triggers an adaptive response called the unfolded protein response (UPR) to restore ER homeostasis (Ron and Walter, 2007). The UPR pathway is also required to maintain hepatic lipid metabolism (Wang et al., 2012). The UPR is coordinated primarily by three ER transmembrane stress transducers, protein kinase RNA-like ER kinase (PERK), activating transcription factor 6 (ATF6) and inositol requiring enzyme 1 (IRE1).

Prolonged ER stress leads to PERK signaling-mediated upregulation of CHOP, a pro-apoptotic transcription factor (Tabas and Ron, 2011; van Galen et al., 2014). One mechanism by which CHOP induces apoptosis is via inhibition of B-cell lymphoma-2 (Bcl-2) expression and induction of bcl-2-like protein 11 (Bim) expression (McCullough et al., 2001; Puthalakath et al., 2007). ATF6 is a membrane-bound transcription factor, but it is cleaved to release its cytoplasmic

domain in response to ER stress. Cleaved ATF6 transcriptionally activates XBP1. XBP1 mRNA is spliced by IRE1 during ER stress to produce the transcription factor, XBP1s (Ron and Walter, 2007). These ER stress-related transcription factors are involved in activation of various ER chaperones and folding-related proteins that directly execute protein quality control (Lee et al., 2003; Hebert and Molinari, 2007).

Glucose-regulated protein 78 (GRP78, also known as BiP) and glucose-regulated protein 94 (GRP94) are molecular chaperones regulating protein quality control and degradation. GRP78 also plays a pivotal role in activation of the UPR, in which GRP78 is released from PERK, IRE1 and ATF6 and activates them. The lectin calnexin is a transmembrane ER chaperone involved in folding of newly synthesized glycoproteins (Coe et al., 2008).

Protein disulfide isomerase (PDI) is a member of PDI superfamily that is involved in oxidative protein folding (Rutkevich and Williams, 2011). ER protein 72 (ERp72) and ER protein 44 (ERp44) are also oxidoreductases in the ER belonging to the PDI family (Määttänen et al., 2010). ER oxireductin 1 (Ero1)-Lα is an oxidase activated during UPR (Harding et al., 2003; Sevier and Kaiser, 2008).

The intrinsic pathway to apoptosis predominantly leads to cytochrome *c* release from the mitochondria into the cytosol. The intrinsic pathway is strictly controlled by anti-apoptotic (Bcl-2 and myeloid cell leukemia-1 (Mcl-1)) and pro-apoptotic (such as Bim and bcl-2 homologous antagonist/killer (Bak)) Bcl-2 family proteases. The extrinsic pathway to apoptosis can bypass the mitochondrial step. The intrinsic and extrinsic pathways activate caspase-3 protease, which is central to execution of apoptosis (Youle and Strasser, 2008). Poly (ADP-ribose) polymerase (PARP) is a cellular substrate of caspases. Cleavage of PARP is considered to be an apoptosis marker (Tewari et al., 1995).

Autophagy is an intracellular pathway responsible for turnover of long-lived proteins (Komatsu et al., 2010). Beclin1 regulates autophagy, forming a multiprotein complex that initiates autophagosome formation (Itakura et al., 2008). Autophagy protein 16L1 (ATG16L1) mediates conjugation between autophagy protein 5 (ATG5) and autophagy protein 12 (ATG12) and delivers this complex to autophagosomes. ATG5-ATG12 conjugates convert the cytoplasmic form of microtubule-associated proteins 1A/1B light chain 3 (LC3-I) to the membrane-bound form, referred to as LC3-II. The conversion of LC3-I to LC3-II is a pivotal process for

maturation of autophagosomes, enabling their fusion with lysosomes and autophagosome cargo degradation (Fujita et al., 2008). The protein p62 is a selective substrate for autophagy (Komatsu et al., 2007, 2010).

Recent evidence suggests the involvement of ER stress and the UPR in development of many chronic liver diseases such as NAFLD (Puri et al., 2008; Hotamisligil, 2010; Li et al., 2012; Pagliassotti, 2012; Lake et al., 2014; Zhou and Liu, 2014). Inadequate response to ER stress may cause fat accumulation, insulin resistance, inflammation, autophagy and apoptosis, all of which are critical to pathogenesis of NAFLD (Cao and Kaufman, 2013; Hou et al., 2014). In my study, expression of various proteins associated with ER stress, autophagy and apoptosis was analyzed in NAFL and NASH tissues to elucidate the roles of those proteins in pathogenesis of the critical metabolic disorder.

2. Materials and methods

2.1. Chemicals

All chemicals used in this study were of reagent grade or higher and were purchased from Sigma-Aldrich (St. Louis, MO, U.S.A.), unless otherwise specified.

2.2. Liver tissues

Frozen human liver tissues were obtained from the National Institutes of Health-funded Liver Tissue Cell Distribution System at the University of Minnesota, Virginia Commonwealth University and the University of Pittsburgh (Fisher et al., 2009). Patient IDs for the liver tissues used are listed in Table 1. Clinical, histopathological, and donor information for the tissues was described previously (Fisher et al., 2009).

2.3. Tissue subcellular fractionation

Subcellular extraction of the liver tissues was performed as described by Cox and Emili (2006). Briefly, tissues were homogenized using a tight-fitting Teflon pestle in ice-cold lysis buffer containing 250 mM sucrose, 50 mM Tris-HCl (pH 7.4), 5

mM $MgCl_2$, 1 mM dithiothreitol (DTT) and 1 mM phenylmethylsulfonyl fluoride (PMSF). The lysate was centrifuged at 6,000 x g for 15 min at 4°C and the pellet resuspended to obtain mitochondrial proteins solubilized in extraction buffer containing 20 mM Tris-HCl (pH 7.8), 0.4 M NaCl, 15% glycerol, 1 mM DTT, 1 mM PMSF and 1.5% Triton-X-100. The supernatant was centrifuged at 100,000 x g for 1 h at 4°C, and the pellet resuspended to extract microsomal proteins into the extraction buffer. Protein concentrations were determined with a BCA protein assay kit (Pierce Biotechnology, Rockford, IL, U.S.A.).

2.4. Western blot analysis

Sample preparation and western blotting were performed as previously described (Kim et al., 2014). Anti-ATG5-ATG12 complex (#4180), -ATG16L1 (#8089), -Bak (#12105), -beclin1 (#3495), -Bim (#2933), -Calnexin (#2679), -CHOP (#2895), -cleaved PARP (#9541), -cytochrome *c* (#4280), -Ero1-Lα (#3264), -ERp44 (#3798), -ERp72 (#5033), -GRP94 (#2104), -LC3-I/II (#12741), -Mcl-1 (#5453), -PDI (#3501) and - voltage-dependent anion-selective channel 1 (VDAC1, #4661) antibodies were from Cell Signaling Technology (Beverly, MA, U.S.A.). Anti-β-actin (ab8226), -Bcl-2 (ab692), -cleaved

caspase-3 (ab2302), -glyceraldehyde-3-phosphate dehydrogenase (GAPDH, ab9485), -GRP78 (ab21685) and -p62 (ab56416) antibodies were from Abcam (Cambridge, MA, U.S.A.). Anti-XBP1s (sc-7160) antibody was from Santa Cruz Biotechnology (Santa Cruz, CA, U.S.A.). Anti-cleaved ATF6 (NBP1-40256) antibody was from Novus Biologicals (Littleton, CO, U.S.A.). Horseradish peroxidase-conjugated goat anti-mouse and anti-rabbit immunoglobulin G (IgG) secondary antibodies were from GenDEPOT (Barker, TX, U.S.A.). The blots were developed using a chemiluminescent detection kit (Ab Frontier, Seoul, Republic of Korea). Densitometric quantification of western blot bands was performed using Image J software, version 1.49 (http://rsb.info.nih.gov/ij/index.html).

2.5. Statistics

The nonparametric Mann-Whitney U test was performed to compare specific protein abundances in NASH and normal liver tissue groups (SAS 9.13 statistical program, SAS Institute, Cary, NC, U.S.A.). A P-value of < 0.05 was considered significant.

3. Results

3.1. Enhanced expression of transcription factors associated with ER stress in NASH tissues

Expression of three ER stress-responsive transcription factors was analyzed in NASH, NAFL and normal liver tissues by western blotting (Figure 1). Levels of cleaved ATF6, XBP1s and CHOP were higher in NASH than in normal tissues ($P < 0.05$), suggesting that there was activation of these main UPR transducers in NASH. Levels of cleaved ATF6 appeared to be very low in normal and NAFL tissues. It appeared that CHOP levels in NAFL tissues were between those in NASH and normal tissues. The two NAFL tissues displayed highly variable levels of XBP1s and CHOP.

3.2. Decreased expression of ER chaperones in NASH tissues

In contrast to the enhanced expression of ER stress-associated transcription factors, levels of some ER chaperones were decreased in NASH tissues (Figure 2). Levels of GRP78 and GRP94 were much lower in NASH than in normal tissues ($P < 0.05$; Figure 2A). As found in the whole

tissues, the NASH microsomes had lower levels of GRP78 and GRP94 than did normal microsomes ($P < 0.05$; Figure 2B).

It appeared that levels of GRP78 and GRP94 in the NAFL tissues were between those in NASH and normal tissues. The microsomal levels of the two chaperones in NAFL tissues were as low as in NASH microsomes.

The NASH tissues and their microsomes also had lower calnexin levels, as compared with normal tissues and their microsomes, respectively ($P < 0.05$; Figures 2A and 2B). Calnexin levels in the NAFL tissues appeared to be between those in normal and NASH tissues. Levels of calnexin in NAFL microsomes also tended to be between those in normal and NASH microsomes.

3.3. Dysregulated expression of protein foldases in NASH tissues

Levels of some enzymes related to protein folding were lower in NASH than in normal tissues. There were lower levels of ER foldases such as PDI, ERp44 and ERp72 in NASH tissues and their microsomes, as compared with in normal tissues and their microsomes, respectively ($P < 0.05$; Figure 3). It appeared that levels of the three foldases in NAFL tissues and microsomes were between those in normal and NASH

samples. However, Ero1-Lα levels were not different among the groups, in either tissues or their microsomes.

3.4. Reduced expression of apoptosis markers in NASH tissues

Cytosolic cytochrome *c* levels were lower in NASH than in normal tissues ($P < 0.05$; Figure 4A), whereas there were no clear differences in cytochrome *c* levels in mitochondria from these two tissue groups. There were also no significant differences in cleaved caspase-3 levels in normal and NASH tissues (Figure 4B). However, cleaved PARP levels were lower in NASH than in normal tissues ($P < 0.05$). It appeared that cleaved PARP levels in NAFL tissues were as high as in the normal tissues.

3.5. Dysregulated expression of Bcl-2 family proteins in NASH tissues

Bcl-2 levels were much higher in NASH than in normal liver tissues ($P < 0.05$; Figure 5A). Bcl-2 levels in NAFL were as low as in the normal tissues. NASH mitochondria also had higher Bcl-2 levels than those of normal ($P < 0.05$) and NAFL tissues (Figure 5B). Bim levels were lower in NASH tissues

and their mitochondria than in the corresponding normal samples ($P < 0.05$). It appeared that expression of the two CHOP-regulated Bcl-2 family proteins was regulated, in NASH tissues, in a manner promoting cell survival.

In contrast to the enhanced expression of Bcl-2, that of Mcl-1, another anti-apoptotic protein, was decreased in NASH tissues and their mitochondria, as compared with in corresponding normal samples ($P < 0.05$). However, it was unclear whether Bak levels were different in NASH and normal tissues or mitochondria.

3.6. Dysregulated expression of autophagy-related proteins

Expression of autophagy-related proteins was also analyzed (Figure 6). The NASH tissues had higher levels of ATG16L1 and LC3-II than the normal tissues ($P < 0.05$). It appeared that LC3-II levels in NAFL tissues were between those in NASH and normal tissues. However, there were no clear differences in levels of beclin1, ATG5-ATG12 conjugate or LC3-I among all tissue groups analyzed. In addition, it appeared that levels of p62 were not different among all tissue groups.

4. Discussion

XBP1s and cleaved ATF6 are among the major UPR transducers (Jiang et al., 2014). Thus, the enhanced expression of XBP1s and cleaved ATF6 in the NASH tissues (Figure 1) suggests that ER stress could be sensed within inflammatory tissues, resulting in UPR activation to restore cellular homeostasis. Induction of XBP1s and cleaved ATF6 was also observed in mouse models of NASH (Rinella et al., 2011; Jung et al., 2014).

Considering that GRP78 expression was increased in mouse NASH tissues (Rinella et al., 2011; González-Rodríguez et al., 2014) as well as in hepatoma cells treated with palmitate (Yamagishi et al., 2012), my observation of decreased GRP78 in NASH tissues (Figure 2) was unexpected. It was reported that the expression level of GRP78 mRNA was lower in human NAFL and NASH tissues than in normal liver tissues (Lake et al., 2014). Notably, GRP78 downregulation occurred in tissues where expression of XBP1s and cleaved ATF6, two transcriptional regulators for GRP78, were induced (Figure 1) (Yoshida et al., 1998; Lee et al., 2003; Ashraf and Sheikh, 2015). Decreased expression of GRP78 was reported in liver tissues of obese db/db mice, in which expression of cleaved ATF6 was

enhanced (Yamagishi et al., 2012).

Inhibition of GRP78 expression may cause fat accumulation in livers of mice. These mice exhibited increased GRP94 levels, PDI, CHOP, XBP1s and cleaved ATF6 (Ji et al., 2011). GRP78 overexpression in the livers of obese ob/ob mice decreased hepatic TG and cholesterol content as well as hepatic expression of XBP1s and ATF6 (Kammoun et al., 2009). Based on these findings, I assumed that decreased GRP78 levels (Figure 2) contributed to the disturbances related to NAFLD and induction of ER stress in liver tissues.

GRP94 depletion did not induce ER stress in the mouse liver, but led to high plasma low-density lipoprotein cholesterol levels (Poirier et al., 2015) as well as to hyperproliferation of mouse liver progenitor cells (Chen et al., 2014). In light of these findings, it is possible that GRP94 downregulation in NASH tissues (Figure 2) is involved in dysfunctional lipid metabolism as well as NASH-related proliferative diseases.

Like those of GRP78, GRP94 and calnexin, levels of the ER-associated protein foldases, PDI, ERp44 and ERp72, were also decreased in NASH tissues (Figure 3). Downregulation of the three foldases was unexpected, based on reports that XBP1s could regulate activation of ERp44 and PDI and that ATF6 could, similarly, activate ERp72 (Yoshida et al., 1998; Wang et

al., 2012; Sha et al., 2014).

It was intriguing that levels of most of the ER related chaperones and foldases analyzed in my study were decreased in NASH tissues (Figures 2 and 3), despite activation of the UPR transducers (Figure 1). Because chaperones and foldases are considered to directly execute protein quality control in the ER, it is possible that capacity for protein quality control was broadly compromised in the ER of NASH tissues.

When ER stress cannot be reversed, the UPR can trigger different pathways leading to cell death, such as apoptosis (Sano and Reed, 2013). However, in my study, levels of two apoptosis markers, cytosolic cytochrome *c* and cleaved PARP, were decreased in NASH tissues (Figure 4), suggesting that apoptotic processes were less active than in normal liver. Apoptosis inhibition does not transform cells. However, when it is combined with activation of growth stimulatory signals, cancers can develop (Gerl and Vaux, 2005).

Activated CHOP can cause changes in gene expression favoring apoptosis, including increased Bim and decreased Bcl-2 expression (Yamaguchi and Wang, 2004; Puthalakath et al., 2007). In contrast to those previously reported observations, CHOP induction (Figure 1) coincided with that of Bcl-2 as well as with inhibition of Bim expression in the NASH tissues

(Figure 5). Based on their activities in apoptotic processes, expression of Bcl-2 and Bim was changed in a manner that would inhibit apoptosis in the NASH tissues. However, expression of another anti-apoptotic regulator, Mcl-1, was changed in a manner that would promote apoptosis. Thus, poorly controlled regulation of Bcl-2 family protein expression may contribute to dysregulation of apoptotic processes in NASH tissues.

Autophagy is a pathway mediating cell survival, although it can also promote cell death under certain conditions. Decreased autophagic function was reported to promote the initial development of NAFLD (Amir and Czaja, 2011). The observation that levels of p62 were unchanged suggests that the autophagy process was not activated in the NASH tissues (Figure 6), even though two major autophagy regulators, ATG16L1 and LC3, were induced.

NAFL may represent an intermediate state leading to NASH, the most extreme form of NAFLD. Five to twenty percent of patients with NAFL progress to NASH (Weiß et al., 2014). Levels of most of the proteins analyzed in NAFL tissues were either similar to those in one of the other two types, NASH and normal, or were somewhere in between (Figures 1-6). That is, NAFL tissues showed no unique expression

patterns of any of the proteins analyzed, as compared with NASH and normal liver tissues.

Taken together, my findings suggest that many proteins related to UPR, apoptosis and autophagy were dysregulated in the NASH tissues. Some of the proteins were dysregulated in NASH tissues in a manner consistent with inhibition of UPR and apoptosis processes. Inhibition of UPR and apoptosis can cause prolonged accumulation of cellular stresses that may, in turn, result in cell transformation. This is interesting to consider because NASH is one of the risk factors for hepatocellular carcinoma. Future studies are warranted to determine tissue environmental factors and signaling pathways that regulate expression of proteins related to UPR and apoptosis in NAFLD tissues.

Table 1. Clinical and donor information for the liver tissues used in this study.

Sample #	Diagnosis	Patient ID	Gender	Age
Normal 1	Normal	D486	Female	58
Normal 2	Normal	D585	Male	60
Normal 3	Normal	D587	Male	49
Normal 4	Normal	UC9113	Female	59
NAFL 1	NAFL	D218	Female	51
NAFL 2	NAFL	UMN1058	Unknown	Unknown
NASH 1	NASH	D346	Female	55
NASH 2	NASH	D515	Female	56
NASH 3	NASH	UMN935	Female	60

NAFL, non-alcoholic fatty liver; NASH, non-alcoholic steatohepatitis

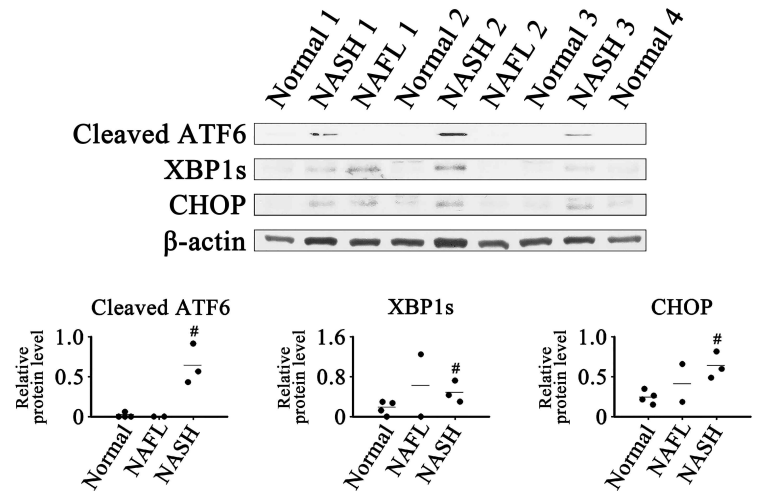

Figure 1. Expression of ER stress-associated transcription factors in NASH, NAFL and normal liver tissues. β-actin was used as an internal control. Horizontal lines represent means of densitometry signals from the western blot analyses for all tissue groups. #, significant differences in signals between NASH and normal liver tissues ($P < 0.05$). Data for NAFL tissues were not used for statistical comparisons because of limited sample number (n = 2).

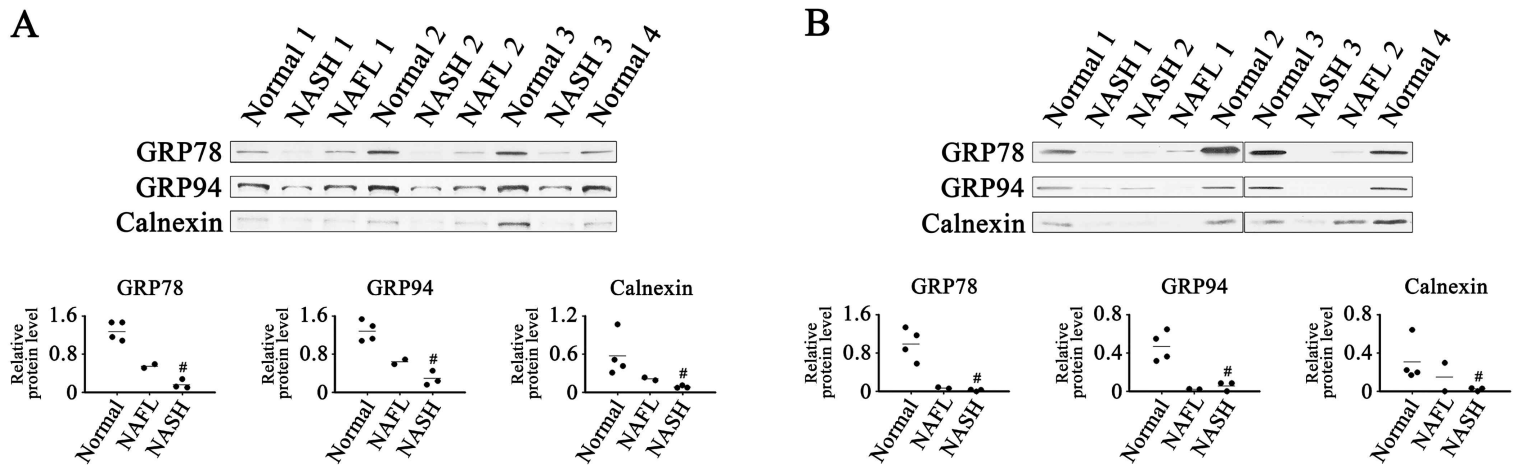

Figure 2. Expression of ER chaperones in NASH, NAFL and normal liver tissues (A) and in their microsomes (B). β-actin was used as an internal control for the whole tissue samples, as described for Figure 1. Horizontal lines represent means of densitometry signals from the western blot analyses for the sample groups. #, significant differences in signals between NASH and normal liver tissues or microsomes ($P < 0.05$). Data for NAFL tissues were not used for statistical comparisons because of limited sample number (n = 2).

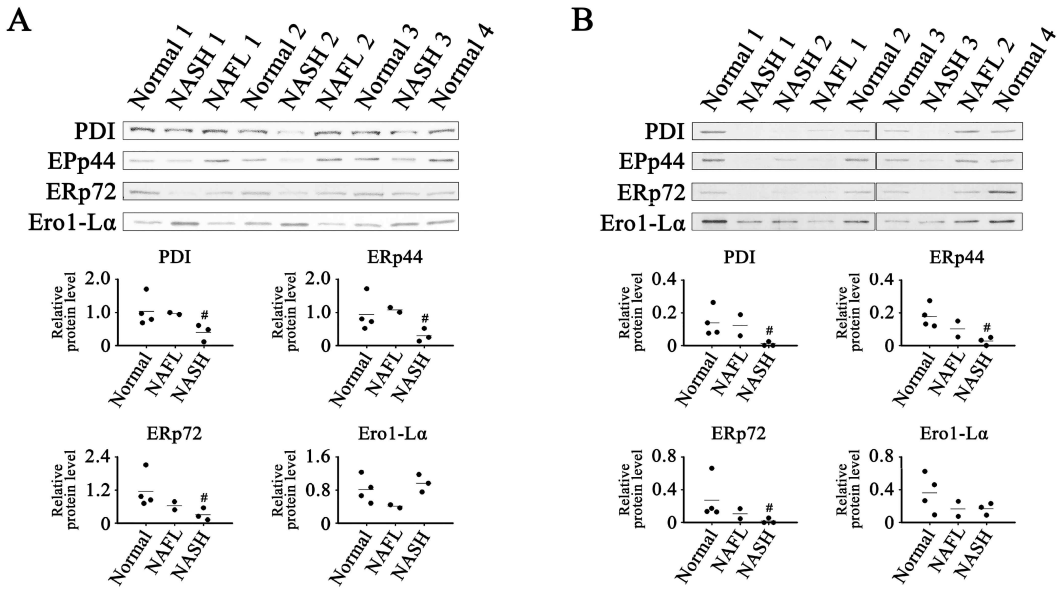

Figure 3. Expression of ER-related foldases in NASH, NAFL and normal liver tissues (A) and in their microsomes (B). β-actin was used as an internal control for the whole tissue samples, as described for Figure 1. Horizontal lines represent means of densitometry signals from the western blot analyses. #, significant differences in signals between NASH and normal liver tissues or microsomes ($P < 0.05$). Data for NAFL tissues were not used for statistical comparisons because of limited sample number (n = 2).

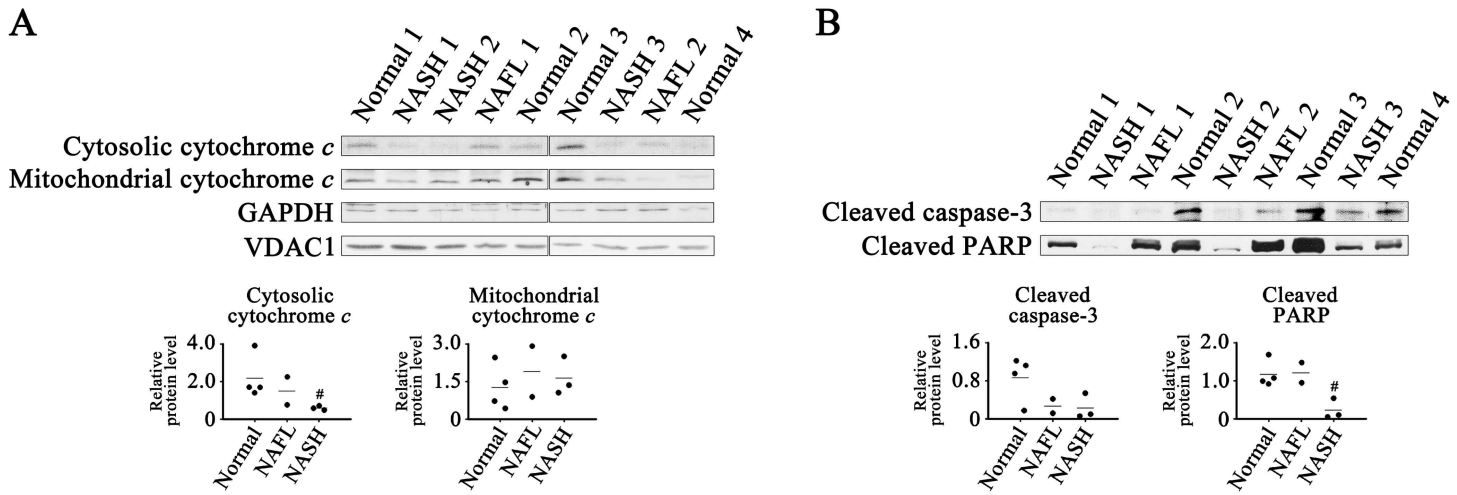

Figure 4. Expression of apoptosis marker proteins in NASH, NAFL and normal liver tissues (A and B). GAPDH and VDAC1 were used as internal controls for cytosolic and mitochondrial samples, respectively (A). β-actin was used as an internal control for the whole tissue samples (B), as described for Figure 1. Horizontal lines represent means of densitometry signals from western blot analyses. #, significant differences in signals between NASH and normal liver tissues ($P < 0.05$). Data for NAFL tissues were not used for statistical comparisons because of limited sample number (n = 2).

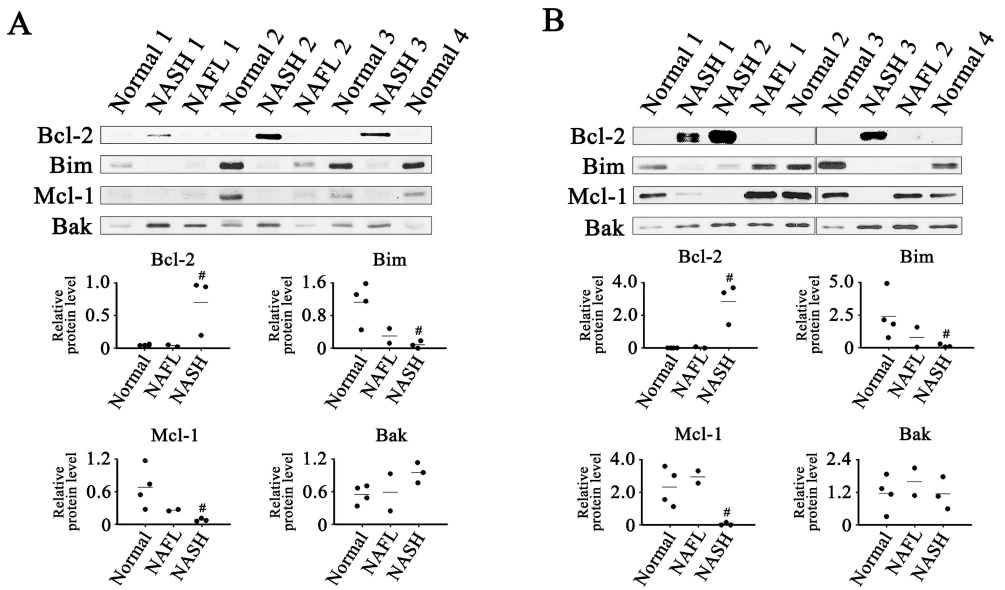

Figure 5. Expression of Bcl-2 family proteins in NASH, NAFL and normal liver tissues (A) and in their mitochondria (B). β-actin and VDAC1 were used as internal controls for the whole tissue and mitochondria samples, as described for Figures 1 and 4, respectively. Horizontal lines represent means of densitometry signals from the western blot analyses. #, significant differences in signals between NASH and normal liver tissues ($P < 0.05$). Data for NAFL tissues were not used for statistical comparisons because of limited sample number (n = 2).

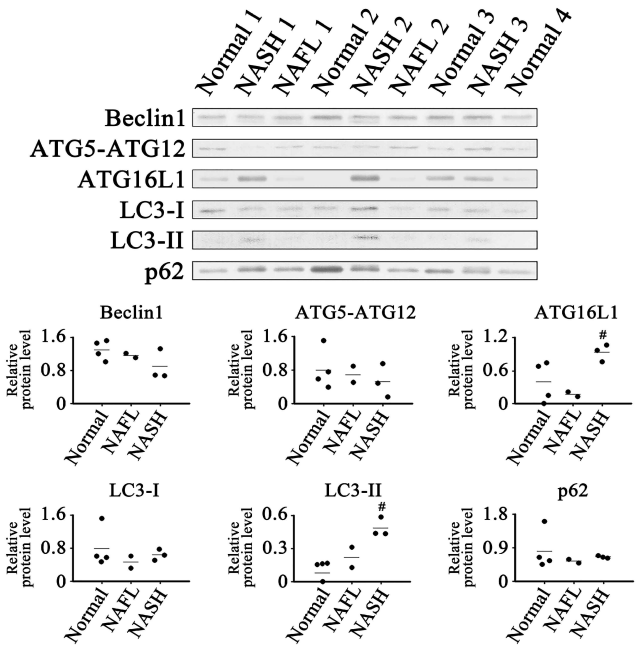

Figure 6. Expression of proteins related to autophagy in NASH, NAFL and normal liver tissues. β-actin was used as internal control, as described for Figure 1. Horizontal lines represent means of densitometry signals from western blot analyses. #, significant differences in signals between NASH and normal liver tissues ($P < 0.05$). Data for NAFL tissues were not used for statistical comparisons because of limited sample number (n = 2).

CHAPTER II

MOLYBDATE ATTENUATES LIPID ACCUMULATION IN THE LIVERS OF MICE FED A DIET DEFICIENT IN METHIONINE AND CHOLINE

1. Introduction

Mo is an essential trace element for mammalian species. Mo is usually bioavailable as molybdate anion in food and water (Mendel and Kruse, 2012). Mo cofactor, a Mo-containing prosthetic group, forms an active site on nearly all mammalian Mo-containing enzymes such as AOX, SUOX, and XDH (Murray et al., 2014).

Hepatic steatosis, or fatty liver, is characterized by the accumulation of lipid droplets, mainly triglyceride (TG), in hepatocytes, and is the consequence of a disturbance in the homeostasis of hepatic lipids (Zhu et al., 2011; Liangpunsakul and Chalasani, 2012). NAFLD is a common chronic liver disease not associated with alcohol use. Patients with NAFLD have a higher prevalence of obesity, insulin resistance, and dyslipidemia. Both perilipin 2 (PLIN2) and PPAR-γ are highly involved in mammalian lipid metabolism, and the expression levels tend to correlate with intracellular lipid accumulation (Motomura et al., 2006; Mwangi et al., 2016).

Oxidative stress refers to an increased production of ROS that cause tissue damage through the oxidation of lipids and proteins. Levels of oxidative damage tend to increase in the livers of mice and humans with NAFLD (Malaguarnera et al.,

2005; Xiao et al., 2015). Cellular antioxidant systems protect cells against oxidative damage by detoxifying ROS (Schumacker, 2015). Superoxide dismutase (SOD) is one of major ROS-scavenging antioxidant enzymes in mammals (Espinosa-Diez et al., 2015). Three isoforms of SODs have been identified in mammals: cytoplasmic Cu/ZnSOD (SOD1), mitochondrial MnSOD (SOD2), and extracellular Cu/ZnSOD (SOD3) (Miao and St Clair, 2009).

Accumulation of unfolded proteins in the ER, called ER stress, activates the UPR. The UPR increases the expression of ER chaperones, such as GRP78, GRP94, and PDI, to upregulate cellular folding capacity (Hetz, 2012). The UPR also induces the expression of CHOP (Zinszner et al., 1998). ER stress and activation of the UPR have been observed in the livers of murine models of NAFLD (González-Rodríguez et al., 2014; Zhang et al., 2016). Oxidative stress and ER stress are two processes that form a vicious cycle in the pathogenesis of NAFLD (Ashraf and Sheikh, 2015). An inadequate response to ER stress may cause fat accumulation and autophagy, both of which are also critical to the development of NAFLD (Cao and Kaufman, 2013; Hou et al., 2014).

Autophagy is an intracellular self-digesting pathway responsible for turnover of long-lived proteins and organelles

(Komatsu et al., 2010). Autophagy also contributes to lipid droplet catabolism, or lipophagy (Singh et al., 2009). Beclin1 regulates an early step in autophagosome formation (Itakura et al., 2008), which is regulated by several proteins, such as autophagy protein 3 (ATG3), ATG5, and autophagy protein 7 (ATG7) (Ichimura et al., 2000; Otomo et al., 2013). The conversion of LC3-I to LC3-II is a critical process for maturation of autophagosomes. The matured autophagosomes fuse with lysosomes to form autolysosomes, the contents of which are degraded, including p62 (Pankiv et al., 2007). Rubicon is a beclin1-interacting negative regulator for autophagosome-lysosome fusion (Matsunaga et al., 2009; Tanaka et al., 2016). Defective autophagy, which is indicated by increased levels of LC3-II as well as by reduced levels of p62, has been implicated in the pathogenesis of NAFLD (Fukuo et al., 2014; González-Rodríguez et al., 2014).

Mice fed a MCD represent a well-established nutritional model of NAFLD. The model has been characterized as increased levels of TG and free fatty acid (FFA) in the liver, as well as a lowered serum TG level. Hepatic signs of autophagic dysfunction and those of increased oxidative damage and ER stress have also been observed in MCD-fed mice (González-Rodríguez et al., 2014; Zhang et al., 2016). Mice given

MCD for about four weeks primarily develop hepatic steatosis, rather than fully established NAFLD, in the liver (González-Rodríguez et al., 2014; Schumacker, 2015; Zhang et al., 2016).

Treatment with SM reduces hepatic levels of TG, cholesterol (CHO), and oxidative damage in diabetic rats (Panneerselvam and Govindasamy, 2004). SM also attenuates chemically induced hepatic steatosis in rats (Eidi et al., 2011). Based upon those previous studies, I evaluated the effects of SM treatment on hepatic steatosis and associated disturbances in a MCD-induced mouse model of hepatic steatosis. SM treatment markedly attenuated hepatic steatosis and oxidative damage, while inducing autophagic processes in the liver.

2. Materials and methods

2.1. Chemicals

All chemicals used in this study were of reagent grade or higher and were purchased from Sigma-Aldrich, unless specified.

2.2. Animal treatments

All animals were used in accordance with the principles outlined in the "Guide for the Care and Use of Laboratory Animals" (National Institutes of Health, U.S.A.). The experimental protocol was approved by the Institutional Animal Care and Use Committees of Seoul National University (Approval #SNU-160503-4-1).

Male C57BL/6 mice were purchased at 9 weeks of age (SLC, Shizuoka, Japan) and housed individually in standard cages in a specific pathogen-free environment controlled for temperature, humidity, and light. The animals were acclimated for 1 week with a chow diet (#5057, Purina, St. Louis, MO, U.S.A.) and plain bottled water *ad libitum*.

Mice were then randomly divided into four groups fed either (1) a chow diet and plain water (Control group), (2)

MCD and plain water (MCD-only group), (3) MCD and water containing 0.3 g/L SM (MCD-low SM group), or (4) MCD and water containing 1.0 g/L SM (MCD-high SM group). The dose level of 1.0 g/L was equivalent to approximately 50 mg Mo/kg body weight/day, considering the animals' body weight and daily water intake that were approximately 24 g and 3 mL/day at the initiation of the treatments, respectively. The SM dose was selected based upon its lowest-observed-adverse-effect-level that was determined in a 90-day study using rats to be 60 mg Mo/kg body weight/day (Murray et al., 2014).

MCD was purchased from Dyets (#518810, Bethlehem, PA, U.S.A.). These interventions were continued for 4 weeks, during which water bottles were changed each week. At the end of the treatment period, mice were fasted for 12 h and euthanized by an intraperitoneal overdose of 2,2,2-tribromoethanol dissolved in tertiary-amyl alcohol. Liver tissues were collected, frozen immediately in liquid nitrogen, and stored at −80°C until use. Portions of liver tissues were fixed in 10% formalin, embedded in paraffin, sectioned, and stained with hematoxylin and eosin (H&E) for histological analysis.

2.3. Serum biochemical analysis

Mouse whole blood was collected by cardiac puncture, incubated for 20 min at room temperature, and then centrifuged at 1,000 x g for 15 min at 4°C to obtain serum. The serum levels of TG, CHO, AST, and ALP were determined using a Hitachi clinical analyzer 7020 (Hitachi, Tokyo, Japan).

2.4. Hepatic lipids

Analysis of hepatic TG contents was performed by tissue saponification in ethanolic potassium hydroxide as described previously (Salmon and Flatt, 1985). Hepatic CHO and FFA were determined using the Total Cholesterol Assay kit (STA-384, Cell Biolabs, San Diego, CA, U.S.A.) and Free Fatty Acid Quantification kit (K612-100, Biovision, Milpitas, CA, U.S.A.), respectively.

2.5. Oxidative stress markers

Levels of malondialdehyde (MDA), a product of lipid peroxidation, were determined using the Oxiselect TBARS assay kit (STA-330, Cell Biolabs). Oxidized protein was detected using the OxyBlot Protein Oxidation Detection kit (S7150, Millipore, Billerica, MA, U.S.A.).

2.6. Enzyme activities

AOX activity was assayed as previously described with the substrate *p*-dimethylaminocinnamaldehyde (Swenson and Casida, 2013). SUOX and XDH activities were determined with sodium sulfite and hypoxanthine as the substrate, respectively (Lee et al., 2002). SOD activity was assayed with the substrate 2-(4-iodophenyl)-3-(4-nitrophenyl)-5-(2,4-disulfophenyl)-2*H*-tetrazolium using a SOD assay kit-WST (S311-10, Dojindo Molecular Technologies, Kumamoto, Japan).

2.7. Western blot analysis

Sample preparation and western blotting were performed as previously described (Lee et al., 2017). Anti-GAPDH (ab9485), -GRP78 (ab21685), -PLIN2 (ab78920) and -p62 (ab56416) antibodies were from Abcam. Anti-ATG3 (#3415), -ATG5 (#12994), -ATG7 (#8588), -beclin1 (#3495), -CHOP (#2895), -GRP94 (#2104), -LC3-I/II (#12741), -PDI (#3501) and -PPAR-ɣ (#2492) antibodies were from Cell Signaling Technology. Horseradish peroxidase-conjugated goat anti-mouse and anti-rabbit IgG secondary antibodies were from GenDEPOT. The blots were developed using a chemiluminescent detection kit (Ab Frontier). Densitometric quantification of western blot bands was performed using Image

J software, version 1.49.

2.7. Immunohistochemistry (IHC)

Paraffin-embedded liver tissue sections (3 μm thick) were deparaffinized in xylene and dehydrated in graded ethanol. For antigen retrieval, sections were heated in 10 mM sodium citrate buffer in a pressure cooker for 20 min. Endogenous peroxidase activity was inactivated with 0.3% hydrogen peroxide for 30 min. After blocking with 2.5% normal horse serum, tissue sections were incubated with anti-p62 antibody for 30 min, followed by incubation with biotinylated anti-mouse IgG antibody (BA-2000, Vector Laboratories, Burlingame, CA, U.S.A.). Color development was performed using the ImmPACT DAB substrate kit (SK-4100, Vector Laboratories), and counterstained with Mayer's hematoxylin.

2.8. Real time RT-PCR

Total RNA was extracted from liver tissues using the PureLink RNA Mini kit (Invitrogen, Carlsbad, CA, U.S.A.). Reverse transcription was performed as previously described (Youn et al., 2009). Real time RT-PCR was performed with gene-specific primers (Table 1) and the EvaGreen qPCR Master

mix (ABM, Richmond, BC, Canada) using a Rotor-Gene Q system (Qiagen, Hilden, Germany). The cDNA samples were denatured initially for 10 min at 95°C and then subjected to an amplification and quantification program repeated 40 times (10 s at 95°C and 30 s at 60°C). Amplification was followed by a melting curve program (72−95°C with a heating rate of 1°C per 5 s and continuous fluorescence measurement).

2.9. Statistics

Statistical analyses were performed using SPSS 23.0 (SPSS, Chicago, IL, U.S.A.). Densitometric data were compared among different groups using a Mann-Whitney U test. All other data are expressed as mean±standard deviation and were analyzed with one-way ANOVA with Tukey's *post hoc* test. A P-value of < 0.05 was considered significant.

3. Results

3.1. SM does not increase the hepatic damage in the MCD-fed mice

Serum AST and ALP, indicators of hepatocellular damage, showed 4.81- and 1.26-fold higher levels in the MCD-only or MCD-fed SM-untreated groups of mice compared with the control or chow diet-fed SM-untreated groups, respectively ($P < 0.05$; Table 2). However, levels of serum AST and ALP were not significantly different among the three MCD-fed mouse groups (MCD-only, MCD-low SM, and MCD-high SM groups). These findings suggest that SM administration does not affect the level of hepatotoxicity induced by MCD.

Serum TG and CHO exhibited 56.3 and 61.3% lower levels in the MCD-only group than in the control group, respectively ($P < 0.05$; Table 2). The level of serum TG was 1.84-fold higher in the MCD-high SM group than the MCD-only group ($P < 0.05$). However, the level of serum CHO was not significantly different among the three groups of MCD-fed mice despite SM administration.

A reduction in body and liver weights was observed in

the MCD-only group, compared with the control group ($P < 0.05$; Table 2). However, SM treatment did not significantly affect body and liver weights in MCD-fed mice. No significant difference in total food intake during the treatment period was observed among the MCD-fed mice (Figure 1).

3.2. SM reduces the TG levels in the MCD-Fed mouse livers

The MCD-only group of mice developed histological changes of hepatic steatosis, such as deposition of lipid vacuoles in hepatocytes (Figure 2A), and exhibited an 8.16-fold higher level of hepatic TG ($P < 0.05$; Figure 2B), compared with the control group. In addition, the expression levels of PPAR-ɣ and PLIN2 were higher in the MCD-only group than in the control group (Figures 2C and 3).

Fat deposition in liver tissues was alleviated after treatment with SM in MCD-fed mice (Figure 2A). Similarly, treatment with high-dose SM reduced hepatic TG levels by 50.5% compared with the MCD-only group ($P < 0.05$; Figure 2B). The expression of PPAR-ɣ and PLIN2 also decreased in MCD-fed mice following SM treatment.

In contrast, SM treatment did not significantly affect levels of hepatic FFA and CHO in the MCD-fed mouse groups

(Figure 2D). The MCD-only group had a 1.82-fold higher level of hepatic FFA and 25.4% lower level of hepatic CHO than the control group ($P < 0.05$).

3.3. SM does not affect the activities of Mo-containing enzyme activities

I analyzed the activities of three Mo-containing oxidases in the liver tissues to determine whether the enzymes contribute to the SM-induced attenuation of steatosis. Hepatic activity of AOX was 64.7% lower in the MCD-only group than in the control group ($P < 0.05$; Figure 4). The activities of SUOX and XDH were 20.1- and 1.54-fold higher, respectively, in the MCD-only group than in the control group ($P < 0.05$). However, the activities of those three enzymes were not significantly different among the three MCD-fed groups.

3.4. SM reduces oxidative damage

The levels of oxidative stress markers were analyzed to study whether SM reduces oxidative damage in the liver of MCD-fed mice. The hepatic level of MDA was 2.20-fold higher in the MCD-only group than in the control group ($P < 0.05$; Figure 5A). However, high-dose SM treatment reduced the

level of hepatic MDA by 55.8% compared with the MCD-only group ($P < 0.05$). The hepatic level of oxidized protein was also reduced after treatment with SM in MCD-fed mice (Figure 5B). The diminished levels of the two oxidative damage markers, MDA and oxidized protein, suggest alleviation of MCD-induced oxidative damage by SM. No apparent differences in oxidized protein levels were observed between the MCD-only and control groups.

Hepatic activity of SOD was 43.5% lower in the MCD-only group than in the control group ($P < 0.05$; Figure 5C). However, high-dose SM treatment increased the hepatic activity of SOD by 1.66-fold compared with the MCD-only group ($P < 0.05$). I also analyzed the mRNA expression of *Sod1*, *Sod2*, and *Sod3* in the liver tissues (Figure 5D). The expression levels of *Sod1* and *Sod2* mRNA were lower in the MCD-only group compared to the control group ($P < 0.05$) which is consistent with another study on MCD-fed mice (Machado et al., 2015). However, the SM treatment did not affect the mRNA expression levels of *Sod1* and *Sod2* in the MCD-fed mice. In addition, there were no significant differences in the *Sod3* mRNA levels among the four groups. These findings suggest that the SM-induced increases of the hepatic SOD activity in the MCD-fed mice (Figure 5C) are not the

result of an increase in the expression of *Sod1*, *Sod2*, and *Sod3* mRNA.

3.5. SM does not affect the expression of ER stress markers

I analyzed the expression of ER stress-related proteins to study whether SM regulates ER stress responses in the liver of MCD-fed mice. Hepatic expression levels of ER stress-related proteins, such as CHOP, GRP78, GRP94, and PDI, were all higher in the MCD-only group than in the control group (Figures 5E and 6). However, no apparent differences in expression of those four proteins were observed among the three MCD-fed groups.

3.6. SM alters the expression of autophagy markers

I also analyzed the expression of autophagy-related proteins to investigate whether SM regulates autophagic processes in the liver of MCD-fed mice. Both LC3-I and LC3-II proteins showed higher levels of expression in the MCD-only group compared with the control group (Figures 7A and 8). The expression level of LC3-I appeared not to change

after treatment with SM in the MCD-fed groups, while that of LC3-II increased following high-dose SM treatment.

Hepatic p62 exhibited a higher expression level in the MCD-only group than in the control group. However, the p62 expression level was reduced after treatment with SM in the MCD-fed mice. IHC analysis also demonstrated SM-induced reduction of p62 protein expression (Figure 7B). The altered expression of autophagy markers LC3-II and p62 suggest that SM activates autophagy processes in liver tissues of MCD-fed mice. However, hepatic expression levels of beclin1, ATG3, ATG5, and ATG7 showed no apparent differences among the four groups of mice (Figures 7A and 8).

I also analyzed the mRNA expression of *Lc3*, *p62*, and *Rubicon* in the liver tissues (Figure 7C). The expression levels of *Lc3* mRNA were higher in the MCD-only group than in the control group ($P < 0.05$), consistent with the protein expression results (Figure 7A). However, SM treatment did not affect the expression levels of *Lc3* mRNA in MCD-fed mice. In addition, there were no significant differences in the expression levels of *p62* mRNA among the four groups of mice. These findings suggest that SM-induced changes in the expression of LC3-II and p62 proteins are unlikely to result from the regulation of mRNA expression. The expression levels for the *Rubicon*

mRNA did not significantly differ among the four groups.

4. Discussion

SM treatment efficiently inhibited MCD-induced accumulation of lipid, principally TG, in the livers (Figure 2). The correlation of PPAR-γ and PLIN2 expression with lipid content in the liver suggests that SM does not disturb lipid metabolism with respect to the regulation of those proteins for which expression is tightly regulated by tissue lipid content (Motomura et al., 2006; Mwangi et al., 2016). In addition, the SM-induced attenuation of hepatic steatosis occurred without affecting the animals' body and liver weights and appetite, as well as without changing the level of hepatocellular damage induced by MCD (Figure 1 and Table 2). These findings suggest that molybdate effectively prevents MCD-induced hepatic steatosis without inducing adverse effects in the liver.

TG stored in lipid droplets is considered inert and therefore harmless to cells; however, FFA is a known mediator of lipid-induced cellular toxicity (Listenberger et al., 2003; Neuschwander-Tetri, 2010). The MCD treatment increased both the TG and FFA levels in the livers, which was accompanied by hepatotoxicity (Figure 2 and Table 2). However, SM administration decreased the TG levels in the livers without affecting the hepatic FFA and damage levels. These findings

suggest that MCD-induced hepatic damage is not mediated by TG but possibly by FFA.

Potential activities of SM as an antioxidant have been demonstrated in previous reports (Ahmed, 2009; Eidi et al., 2011; Ale-Ebrahim et al., 2015). In agreement with these findings, SM was observed to decrease the levels of both MDA and oxidized protein potently. It is likely that molybdate-induced increase of SOD activities (Figure 5) contributed to the attenuation of oxidative damages. Molybdate-induced enhancement of SOD activities was also observed in rat livers (Panneerselvam and Govindasamy, 2004; Eidi et al., 2011). However, it appears that the increase in hepatic SOD activity is not due to an enhanced expression of the *Sod* isoforms.

An increase in lipid peroxidation was observed in the livers of MCD-fed mice (Figure 5), which is consistent with previous studies (Sutti et al., 2014; Zhang et al., 2016). However, the level of protein oxidation was not markedly altered by MCD. The potential causes for the difference in sensitivities to lipid and protein oxidation are unclear.

SM appeared to have no effect on CHO levels among MCD-fed mice (Figure 2 and Table 2). However, CHO levels were reduced to a greater extent in the serum than in the livers of the MCD-only group compared with the control group,

as demonstrated in a previous study (Rizki et al., 2006). These findings suggest MCD-induced disturbances in the tissue distribution of CHO.

Dysregulation of the activities of the two Mo-containing oxidases, SUOX and AOX, may lead to disturbances of the relevant metabolic pathways in the liver of MCD-fed mice (Figure 4). SUOX oxidizes sulfite to sulfate, the last step of metabolism of sulfur-containing compounds (Mendel and Kruse, 2012). It is possible that the dramatic increase of SUOX activity is associated with dysregulated metabolism of sulfur-containing compounds in the deficiency of methionine, an essential sulfur-containing amino acid.

Unresponsiveness to SM treatment in the activity levels of the three Mo-containing oxidases suggests that the activities of those enzymes are unlikely to contribute to molybdate-mediated alleviation of lipid accumulation. It is also unlikely that regulation of ER stress is involved in the molybdate-mediated reduction of lipid accumulation based upon the findings that the expression levels of four ER stress-responsive UPR proteins was not affected by SM (Figure 5).

Autophagy is known to have an important functional role in the breakdown of TG stored in lipid droplets and to increase

the secretion of very low-density lipoprotein-associated TG from rat livers (Singh et al., 2009; Skop et al., 2012). The altered expression of the LC3-II and p62 proteins, without affecting the mRNA levels, indicates the SM-induced activation of the autophagic pathways in the MCD-fed mouse liver (Figure 7). The increased level of serum TG by SM (Table 2) also underlies the activation of autophagy. It is plausible that the molybdate-activated autophagy contributed to the decrease in the lipid deposition in the livers of the MCD-fed mice (Figure 2).

Rubicon is a negative regulator for autophagy and also has a role in enhancing lipid accumulation in the liver of mice fed a high-fat diet (Matsunaga et al., 2009; Tanaka et al., 2016). However, in view of the unresponsiveness of the *Rubicon* expression to the MCD and SM treatments (Figure 7), it is unlikely that *Rubicon* has a functional role in MCD-induced steatosis and its attenuation by molybdate.

Taken together, these findings suggest that molybdate effectively prevents MCD-induced lipid accumulation without causing adverse effects in the mouse liver, and that the lipid catabolic processes may involve the activation of autophagy. Molybdate also contributes to the alleviation of oxidative damage in the livers of MCD-fed mice. In light of the notion

that both lipid accumulation and oxidative stress are major pathologic contributors to the development of NAFLD, molybdate may be useful in the treatment and prevention of NAFLD. To the best of my knowledge, this is the first experimental study to investigate the effects of molybdate in non-alcoholic fatty liver disease, and also the first that demonstrates molybdate-induced autophagy. Future studies are warranted to determine the anti-NAFLD effects of molybdate in other animal models.

Table 1. Specific primers used in real time RT-PCR.

Gene	Forward primer (5′ to 3′)	Reverse primer (5′ to 3′)
β-actin	CCCTGGAGAAGAGCTATGAGC	TTACGGATGTCAACGTCACAC
Lc3	TACAAGGGTGAGAAGCAGCTG	ACACTCACCATGCTGTGC
p62	GGAGCTGACAATGGCTATGT	TGAGCACATGGTGGGCGATG
Rubicon	CCTGGATTCCTTTGACGTGGTT	CAGTTCTCCCTTCTTGGTTGC
Sod1	TTACAGGATTAACTGAAGGCCA	CTGCACTGGTACAGCCTTGT
Sod2	AGGAGCAAGGTCGCTTACAGA	CCACACGTCAATCCCCAGCA
Sod3	TTCTTGTTCTACGGCTTGCTAC	CTCCATCCAGATCTCCAGCACT

Lc3, microtubule-associated proteins 1A/1B light chain 3; *Sod1*, cytoplasmic Cu/Zn superoxide dismutase; *Sod2*, mitochondrial Mn superoxide dismutase; *Sod3*, extracellular Cu/Zn superoxide dismutase.

Table 2. Effects of SM on serum biochemical parameters and weights in MCD-fed mice.

	Control	MCD-only	MCD-low SM	MCD-high SM
AST (IU/L)	300 ± 112 [a]	1442 ±139 [b]	884 ± 440 [a,b]	949 ± 567 [a,b]
ALP (mg/dL)	321 ± 22 [a]	403 ± 31 [b]	436 ± 68 [b]	441 ± 53 [b]
TG (mg/dL)	49 ± 7 [a]	22 ± 3 [b]	26 ± 10 [b]	40 ± 8 [a]
CHO (mg/dL)	89 ± 6 [a]	35 ± 5 [b]	36 ± 10 [b]	47 ± 4 [b]
Body weight (g)	25.6 ± 0.9 [a]	16.4 ± 0.9 [b]	16.8 ± 0.7 [b]	16.0 ± 0.7 [b]
Liver weight (g)	1.30 ± 0.07 [a]	0.70 ± 0.08 [b]	0.73 ± 0.06 [b]	0.68 ± 0.01 [b]

ALP, alkaline phosphatase; AST, aspartate aminotransferase; CHO, cholesterol; MCD, methionine- and choline-deficient diet; SM, sodium molybdate dihydrate; TG, triglyceride.

[a,b] Different letters represent significant differences among groups ($P < 0.05$, Tukey's *post hoc* test).

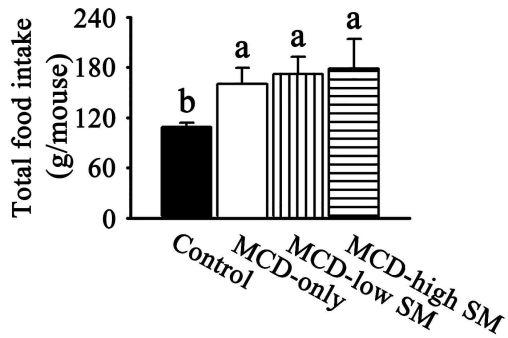

Figure 1. Total food intake over 4 weeks in mice fed a control diet or MCD diet. Different letters above bars represent significant differences among groups (n = 4−5, Tukey's *post hoc* test, $P < 0.05$).

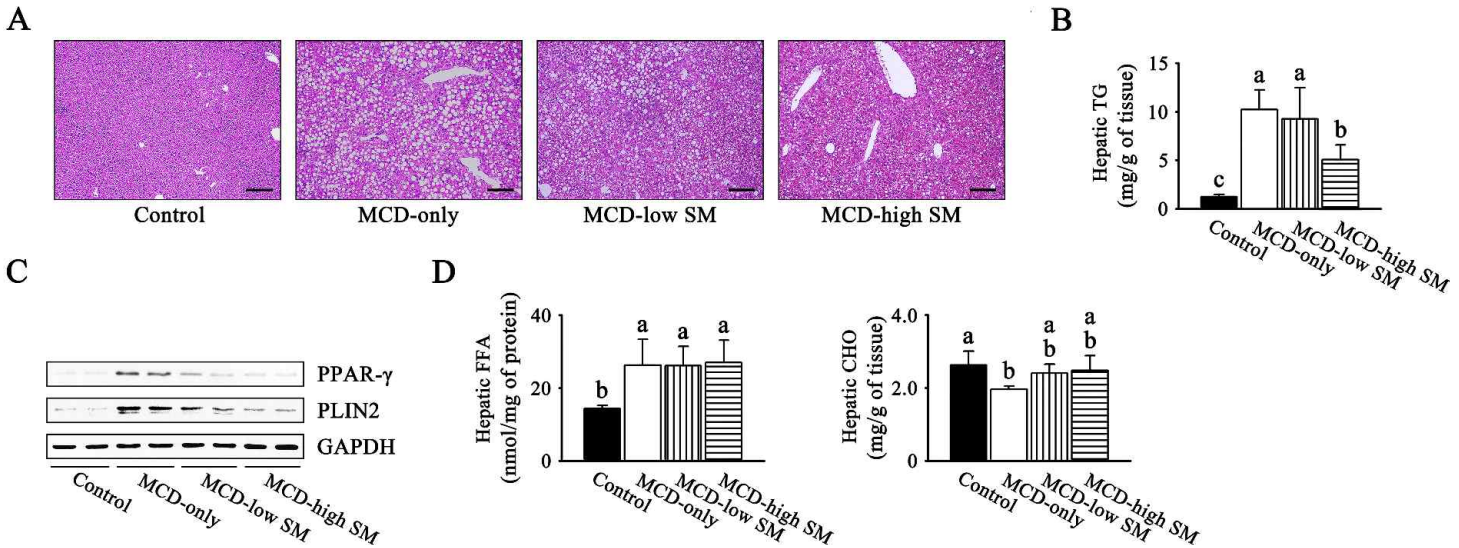

Figure 2. Effects of SM on development of hepatic steatosis in MCD-fed mice. Male C57BL/6 mice at 10 weeks of age were fed MCD and bottled water containing SM (0.3 and 1.0 g/L) for four weeks. (A) H&E-stained liver sections. Scale bars, 200 μm. (B) Hepatic TG content. (C) Hepatic expression of lipid accumulation-related proteins. GAPDH was used as an internal control. (D) Hepatic contents of FFA and CHO. Groups with the same alphabet label above the bars in panels B and D are not statistically different from each other; groups with different labels are statistically different (n = 4−5, Tukey's *post hoc* test, $P < 0.05$).

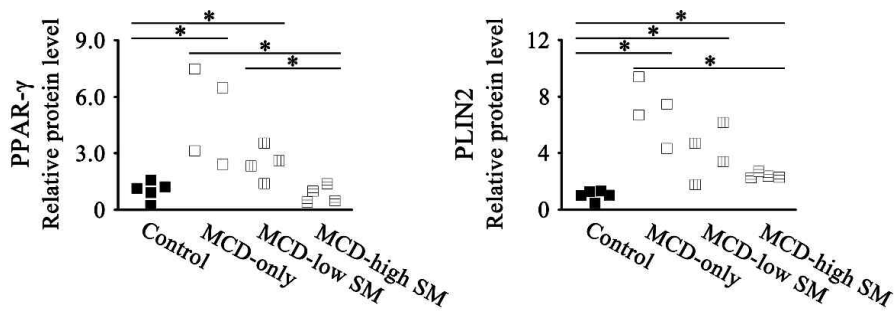

Figure 3. Densitometric analysis for western blots in Figure 2C. Asterisks indicate significant differences between the two groups at either end of the horizontal lines ($P < 0.05$, Mann-Whitney U test).

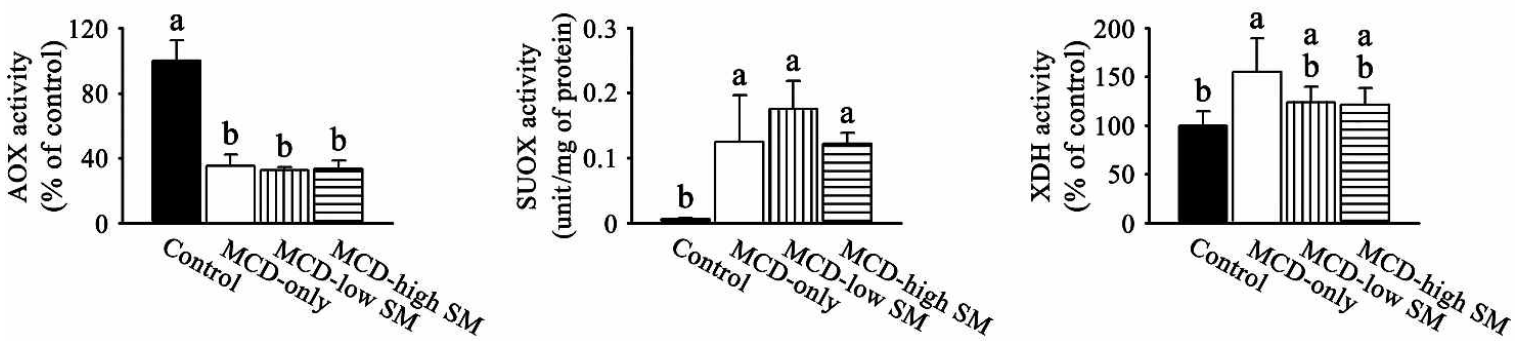

Figure 4. Effects of SM on the activity levels of Mo-containing oxidases in liver tissues of MCD-fed mice. Male C57BL/6 mice at 10 weeks of age were fed MCD and bottled water containing SM (0.3 and 1.0 g/L) for four weeks. Groups with the same alphabet label above the bars are not statistically different from each other; groups with different labels are statistically different (n = 4−5, Tukey's *post hoc* test, $P < 0.05$).

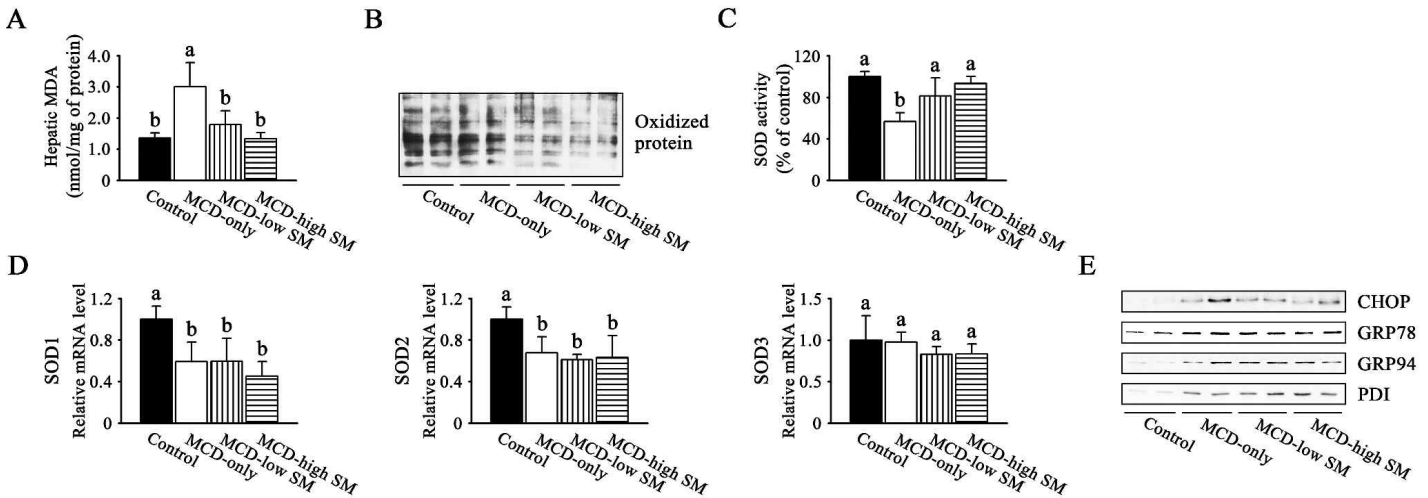

Figure 5. Effects of SM on oxidative stress and ER stress in liver tissues of MCD-fed mice. Male C57BL/6 mice at 10 weeks of age were fed MCD and bottled water containing SM (0.3 and 1.0 g/L) for four weeks. (A) Hepatic MDA content. (B) Hepatic expression of oxidized protein. (C) Hepatic activity of SOD. (D) Hepatic expression of *Sod1*, *Sod2* and *Sod3* mRNA. mRNA expression levels are normalized to *β-actin* and expressed relative to the control group set at 1.0. (E) Hepatic expression of ER stress-related proteins. GAPDH was used as an internal control shown in Figure 2C. Groups with the same alphabet label above the bars in panels A, C and D are not statistically different from each other; groups with different labels are statistically different (n = 4–5, Tukey's *post hoc* test, $P < 0.05$).

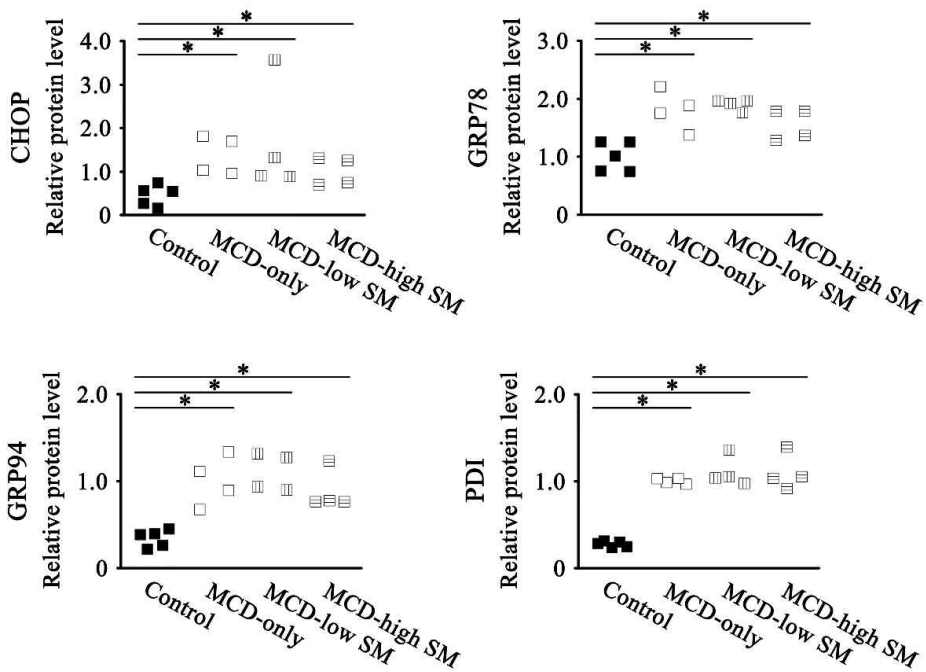

Figure 6. Densitometric analysis for western blots in Figure 5D. Asterisks indicate significant differences between the two groups at either end of the horizontal lines ($P < 0.05$, Mann-Whitney U test).

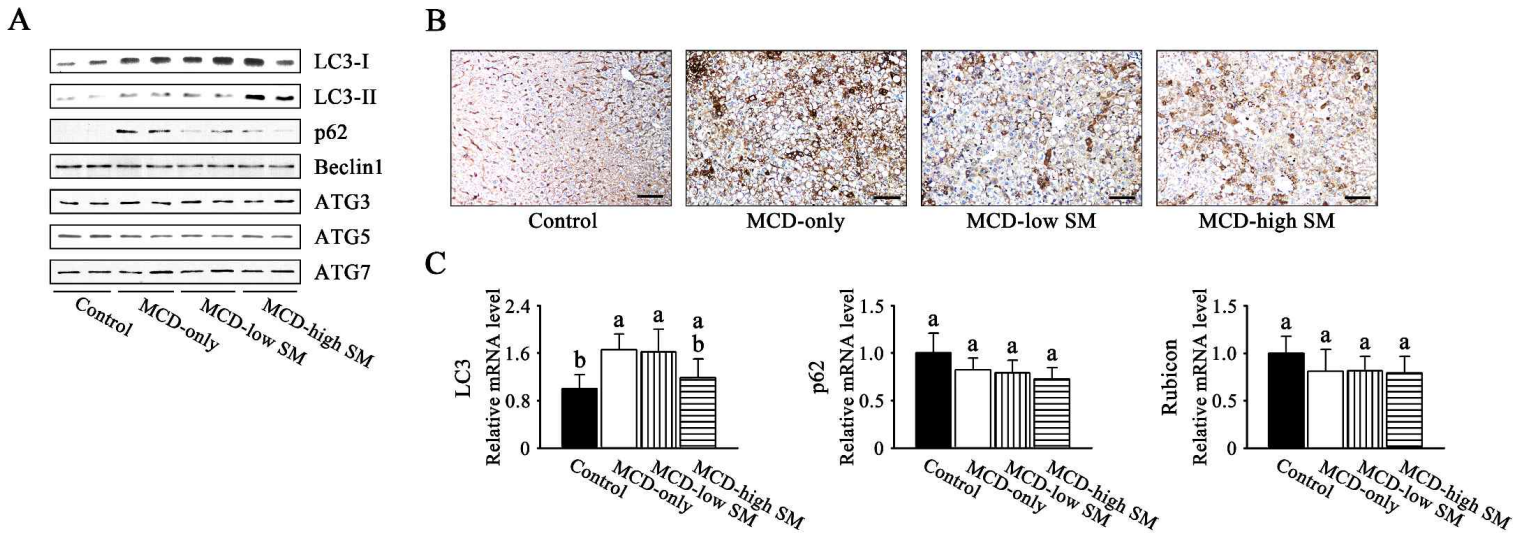

Figure 7. Effects of SM on the autophagic pathway in liver tissues of MCD-fed mice. Male C57BL/6 mice at 10 weeks of age were fed MCD and bottled water containing SM (0.3 and 1.0 g/L) for four weeks. (A) Hepatic expression of autophagy-related proteins. GAPDH was used as an internal control, as shown in Figure 2C. (B) IHC analysis of p62 protein in liver sections. Scale bars, 200 μm. (C) Hepatic mRNA expression of *Lc3*, *p62* and *Rubicon*. mRNA expression levels are normalized to *β-actin* and expressed relative to the control group set at 1.0. Groups with the same alphabet label above the bars in panel C are not statistically different from each other; groups with different labels are statistically different (n = 4–5, Tukey's *post hoc* test, $P < 0.05$).

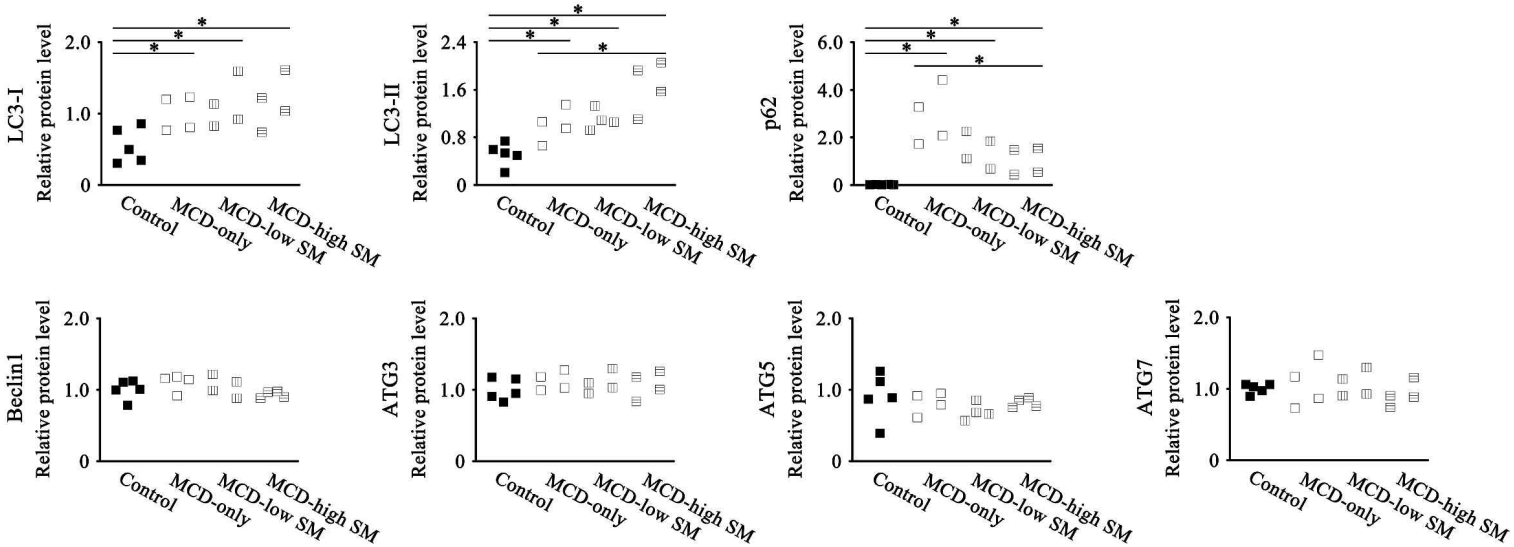

Figure 8. Densitometric analysis for western blots in Figure 7A. Asterisks indicate significant differences between the two groups at either end of the horizontal lines ($P < 0.05$, Mann-Whitney U test).

REFERENCES

Ahmed AA. Beneficial effects of combined administration of sodium molybdate with atorvastatin in hyperlipidemic hamsters. Drug Discov Ther. 2009; 3:62-70.

Ale-Ebrahim M, Eidi A, Mortazavi P, Tavangar SM, Tehrani DM. Hepatoprotective and antifibrotic effects of sodium molybdate in a rat model of bile duct ligation. J Trace Elem Med Biol. 2015; 29:242-248.

Amir M, Czaja MJ. Autophagy in nonalcoholic steatohepatitis. Expert Rev Gastroenterol Hepatol. 2011; 5:159-166.

Angulo P, Keach JC, Batts KP, Lindor KD. Independent predictors of liver fibrosis in patients with nonalcoholic steatohepatitis. Hepatology. 1999; 30:1356-1362.

Anke M, Groppel B, Arnhold W, Langer M, Krause U. The influence of the ultra trace element deficiency (Mo, Ni, As, Cd, V) on growth, reproduction performance and life expectancy. In: TOMITA H., ed. Trace Elements in Clinical Medicine.

Springer-Verlag Tokyo, 1990; 361-376.

Armstrong MJ, Gaunt P, Aithal GP, Barton D, Hull D, Parker R, Hazlehurst JM, Guo K; LEAN trial team, Abouda G, Aldersley MA, Stocken D, Gough SC, Tomlinson JW, Brown RM, Hübscher SG, Newsome PN. Liraglutide safety and efficacy in patients with non-alcoholic steatohepatitis (LEAN): a multicentre, double-blind, randomised, placebo-controlled phase 2 study. Lancet. 2016; 387:679-690.

Arsov T, Silva DG, O'Bryan MK, Sainsbury A, Lee NJ, Kennedy C, Manji SS, Nelms K, Liu C, Vinuesa CG, de Kretser DM, Goodnow CC, Petrovsky N. Fat aussie--a new Alström syndrome mouse showing a critical role for ALMS1 in obesity, diabetes, and spermatogenesis. Mol Endocrinol. 2006; 20:1610-1622.

Arun J, Clements RH, Lazenby AJ, Leeth RR, Abrams GA. The prevalence of nonalcoholic steatohepatitis is greater in morbidly obese men compared to women. Obes Surg. 2006; 16:1351-1358.

Ascha MS, Hanouneh IA, Lopez R, Tamimi TA, Feldstein AF, Zein NN. The incidence and risk factors of hepatocellular

carcinoma in patients with nonalcoholic steatohepatitis. Hepatology. 2010; 51:1972-1978.

Ashraf NU, Sheikh TA. Endoplasmic reticulum stress and Oxidative stress in the pathogenesis of Non-alcoholic fatty liver disease. Free Radic Res. 2015; 49:1405-1418.

Beers MH, Berkow R, eds. The Merck Manual of Diagnosis and Therapy. 17th edition. White house Station, NJ: Merck Research Laboratories, 1999: 55.

Belfort R, Harrison SA, Brown K, Darland C, Finch J, Hardies J, Balas B, Gastaldelli A, Tio F, Pulcini J, Berria R, Ma JZ, Dwivedi S, Havranek R, Fincke C, DeFronzo R, Bannayan GA, Schenker S, Cusi K. A placebo-controlled trial of pioglitazone in subjects with nonalcoholic steatohepatitis. N Engl J Med. 2006; 355:2297-2307.

Bortels H. Molybdän als Katalysator bei der biologischen Stickstoffbindung. Arch Mikrobiol. 1930; 1:333-342.

Bourke CA. Molybdenum Deficiency Produces Motor Nervous Effects That Are Consistent with Amyotrophic Lateral

Sclerosis. Front Neurol. 2016; 7:28.

Brewer GJ, Askari F, Dick RB, Sitterly J, Fink JK, Carlson M, Kluin KJ, Lorincz MT. Treatment of Wilson's disease with tetrathiomolybdate: V. Control of free copper by tetrathiomolybdate and a comparison with trientine. Transl Res. 2009; 154:70-77.

Bugianesi E, Gentilcore E, Manini R, Natale S, Vanni E, Villanova N, David E, Rizzetto M, Marchesini G. A randomized controlled trial of metformin versus vitamin E or prescriptive diet in nonalcoholic fatty liver disease. Am J Gastroenterol. 2005; 100:1082-1090.

Cao SS, Kaufman RJ. Targeting endoplasmic reticulum stress in metabolic disease. Expert Opin Ther Targets. 2013; 17:437-448.

Chalasani N, Younossi Z, Lavine JE, Diehl AM, Brunt EM, Cusi K, Charlton M, Sanyal AJ. The diagnosis and management of non-alcoholic fatty liver disease: practice Guideline by the American Association for the Study of Liver Diseases, American College of Gastroenterology, and the American Gastroenterological Association. Hepatology. 2012; 55:2005-2023.

Chen CH, Huang MH, Yang JC, Nien CK, Yang CC, Yeh YH, Yueh SK. Prevalence and risk factors of nonalcoholic fatty liver disease in an adult population of taiwan: metabolic significance of nonalcoholic fatty liver disease in nonobese adults. J Clin Gastroenterol. 2006; 40:745-752.

Chen WT, Tseng CC, Pfaffenbach K, Kanel G, Luo B, Stiles BL, Lee AS. Liver-specific knockout of GRP94 in mice disrupts cell adhesion, activates liver progenitor cells, and accelerates liver tumorigenesis. Hepatology. 2014; 59:947-957.

Clarke JD, Novak P, Lake AD, Shipkova P, Aranibar N, Robertson D, Severson PL, Reily MD, Futscher BW, Lehman-McKeeman LD, Cherrington NJ. Characterization of hepatocellular carcinoma related genes and metabolites in human nonalcoholic fatty liver disease. Dig Dis Sci. 2014; 59:365-374.

Coe H, Bedard K, Groenendyk J, Jung J, Michalak M. Endoplasmic reticulum stress in the absence of calnexin. Cell Stress Chaperones. 2008; 13:497-507.

Cohen HJ, Drew RT, Johnson JL, Rajagopalan KV. Molecular basis of the biological function of molybdenum: the relationship

between sulfite oxidase and the acute toxicity of bisulfite and SO2. Proc Natl Acad Sci U S A. 1973; 70:3655-3659.

Cox B, Emili A. Tissue subcellular fractionation and protein extraction for use in mass-spectrometry-based proteomics. Nat Protoc. 2006; 1:1872-1878.

Day CP, James OF. Steatohepatitis: a tale of two "hits"? Gastroenterology. 1998; 114:842-845.

Deosthale YG, Gopalan C. The effect of molybdenum levels in sorghum (Sorghum vulgare Pers.) on uric acid and copper excretion in man. Br J Nutr. 1974; 31:351-355.

Dyson JK, Anstee QM, McPherson S. Non-alcoholic fatty liver disease: a practical approach to diagnosis and staging. Frontline Gastroenterol. 2014; 5:211-218.

Eguchi Y, Hyogo H, Ono M, Mizuta T, Ono N, Fujimoto K, Chayama K, Saibara T; JSG-NAFLD. Prevalence and associated metabolic factors of nonalcoholic fatty liver disease in the general population from 2009 to 2010 in Japan: a multicenter large retrospective study. J Gastroenterol. 2012; 47:586-595.

Eidi A, Eidi M, Al-Ebrahim M, Rohani AH, Mortazavi P. Protective effects of sodium molybdate on carbon tetrachloride-induced hepatotoxicity in rats. J Trace Elem Med Biol. 2011; 25:67-71.

Espinosa-Diez C, Miguel V, Mennerich D, Kietzmann T, Sánchez-Pérez P, Cadenas S, Lamas S. Antioxidant responses and cellular adjustments to oxidative stress. Redox Biol. 2015; 6:183-197.

Fan H, Pan Q, Xu Y, Yang X. Exenatide improves type 2 diabetes concomitant with non-alcoholic fatty liver disease. Arq Bras Endocrinol Metabol. 2013; 57:702-708.

Fan JG, Zhu J, Li XJ, Chen L, Lu YS, Li L, Dai F, Li F, Chen SY. Fatty liver and the metabolic syndrome among Shanghai adults. J Gastroenterol Hepatol. 2005; 20:1825-1832.

Farrell GC, Larter CZ. Nonalcoholic fatty liver disease: from steatosis to cirrhosis. Hepatology. 2006; 43:S99-S112.

Feldstein AE, Canbay A, Angulo P, Taniai M, Burgart LJ, Lindor KD, Gores GJ. Hepatocyte apoptosis and fas expression

are prominent features of human nonalcoholic steatohepatitis. Gastroenterology. 2003; 125:437-443.

Fisher CD, Lickteig AJ, Augustine LM, Ranger-Moore J, Jackson JP, Ferguson SS, Cherrington NJ. Hepatic cytochrome P450 enzyme alterations in humans with progressive stages of nonalcoholic fatty liver disease. Drug Metab Dispos. 2009; 37:2087-2094.

Flora SJS, Jeevaratnam K, Kumar D. Proventive effects of sodium molybdate in lead intoxication in rats. Ecotoxicology and Environmental Safety. 1993; 26:133-137.

Fransen M, Nordgren M, Wang B, Apanasets O. Role of peroxisomes in ROS/RNS-metabolism: implications for human disease. Biochim Biophys Acta. 2012; 1822:1363-1373.

Frith J, Day CP, Henderson E, Burt AD, Newton JL. Non-alcoholic fatty liver disease in older people. Gerontology. 2009; 55:607-613.

Fujita N, Itoh T, Omori H, Fukuda M, Noda T, Yoshimori T. The Atg16L complex specifies the site of LC3 lipidation for

membrane biogenesis in autophagy. Mol Biol Cell. 2008; 19:2092-2100.

Fujita N, Miyachi H, Tanaka H, Takeo M, Nakagawa N, Kobayashi Y, Iwasa M, Watanabe S, Takei Y. Iron overload is associated with hepatic oxidative damage to DNA in nonalcoholic steatohepatitis. Cancer Epidemiol Biomarkers Prev. 2009; 18:424-432.

Fukuo Y, Yamashina S, Sonoue H, Arakawa A, Nakadera E, Aoyama T, Uchiyama A, Kon K, Ikejima K, Watanabe S. Abnormality of autophagic function and cathepsin expression in the liver from patients with non-alcoholic fatty liver disease. Hepatol Res. 2014; 44:1026-1036.

Gartner EM, Griffith KA, Pan Q, Brewer GJ, Henja GF, Merajver SD, Zalupski MM. A pilot trial of the anti-angiogenic copper lowering agent tetrathiomolybdate in combination with irinotecan, 5-flurouracil, and leucovorin for metastatic colorectal cancer. Invest New Drugs. 2009; 27:159-165.

Gerl R, Vaux DL. Apoptosis in the development and treatment of cancer. Carcinogenesis. 2005; 26:263-270.

Giannini EG, Testa R, Savarino V. Liver enzyme alteration: a guide for clinicians. CMAJ. 2005; 172:367-379.

González-Rodríguez A, Mayoral R, Agra N, Valdecantos MP, Pardo V, Miquilena-Colina ME, Vargas-Castrillón J, Lo Iacono O, Corazzari M, Fimia GM, Piacentini M, Muntané J, Boscá L, García-Monzón C, Martín-Sanz P, Valverde ÁM. Impaired autophagic flux is associated with increased endoplasmic reticulum stress during the development of NAFLD. Cell Death Dis. 2014; 5:e1179.

Green DR, Reed JC. Mitochondria and apoptosis. Science. 1998; 281:1309-1312.

Grunden AM, Shanmugam KT. Molybdate transport and regulation in bacteria. Arch Microbiol. 1997; 168:345-354.

Han J, Kaufman RJ. The role of ER stress in lipid metabolism and lipotoxicity. J Lipid Res. 2016; 57:1329-1338.

Hänzelmann P, Schwarz G, Mendel RR. Functionality of alternative splice forms of the first enzymes involved in human molybdenum cofactor biosynthesis. J Biol Chem. 2002;

277:18303-18312.

Harding HP, Zhang Y, Zeng H, Novoa I, Lu PD, Calfon M, Sadri N, Yun C, Popko B, Paules R, Stojdl DF, Bell JC, Hettmann T, Leiden JM, Ron D. An integrated stress response regulates amino acid metabolism and resistance to oxidative stress. Mol Cell. 2003; 11:619-633.

Hardwick RN, Fisher CD, Canet MJ, Lake AD, Cherrington NJ. Diversity in antioxidant response enzymes in progressive stages of human nonalcoholic fatty liver disease. Drug Metab Dispos. 2010; 38:2293-2301.

Haring R, Wallaschofski H, Nauck M, Dörr M, Baumeister SE, Völzke H. Ultrasonographic hepatic steatosis increases prediction of mortality risk from elevated serum gamma-glutamyl transpeptidase levels. Hepatology. 2009; 50:1403-1411.

Hebert DN, Molinari M. In and out of the ER: protein folding, quality control, degradation, and related human diseases. Physiol Rev. 2007; 87:1377-1408.

Hetz C. The unfolded protein response: controlling cell fate

decisions under ER stress and beyond. Nat Rev Mol Cell Biol. 2012; 13:89-102.

Hotamisligil GS. Endoplasmic reticulum stress and the inflammatory basis of metabolic disease. Cell. 2010; 140:900-917.

Hou NS, Gutschmidt A, Choi DY, Pather K, Shi X, Watts JL, Hoppe T, Taubert S. Activation of the endoplasmic reticulum unfolded protein response by lipid disequilibrium without disturbed proteostasis in vivo. Proc Natl Acad Sci U S A. 2014; 111:E2271-E2280.

Hussain M, Majeed Babar MZ, Hussain MS, Akhtar L. Vildagliptin ameliorates biochemical, metabolic and fatty changes associated with non alcoholic fatty liver disease. Pak J Med Sci. 2016; 32:1396-1401.

Hutzler JM, Yang YS, Albaugh D, Fullenwider CL, Schmenk J, Fisher MB. Characterization of aldehyde oxidase enzyme activity in cryopreserved human hepatocytes. Drug Metab Dispos. 2012; 40:267-275.

Ichimura Y, Kirisako T, Takao T, Satomi Y, Shimonishi Y,

Ishihara N, Mizushima N, Tanida I, Kominami E, Ohsumi M, Noda T, Ohsumi Y. A ubiquitin-like system mediates protein lipidation. Nature. 2000; 408:488-492.

Ikawa-Yoshida A, Matsuo S, Kato A, Ohmori Y, Higashida A, Kaneko E, Matsumoto M. Hepatocellular carcinoma in a mouse model fed a choline-deficient, L-amino acid-defined, high-fat diet. Int J Exp Pathol. 2017; 98:221-233.

Ip E, Farrell G, Hall P, Robertson G, Leclercq I. Administration of the potent PPARalpha agonist, Wy-14,643, reverses nutritional fibrosis and steatohepatitis in mice. Hepatology. 2004; 39:1286-1296.

Itakura E, Kishi C, Inoue K, Mizushima N. Beclin 1 forms two distinct phosphatidylinositol 3-kinase complexes with mammalian Atg14 and UVRAG. Mol Biol Cell. 2008; 19:5360-5372.

Ives A, Nomura J, Martinon F, Roger T, LeRoy D, Miner JN, Simon G, Busso N, So A. Xanthine oxidoreductase regulates macrophage IL1β secretion upon NLRP3 inflammasome activation. Nat Commun. 2015; 6:6555.

Jakubiczka-Smorag J, Santamaria-Araujo JA, Metz I, Kumar A, Hakroush S, Brueck W, Schwarz G, Burfeind P, Reiss J, Smorag L. Mouse model for molybdenum cofactor deficiency type B recapitulates the phenotype observed in molybdenum cofactor deficient patients. Hum Genet. 2016; 135:813-826.

Jarrell WM, Page AL, Elseewi AA. Molybdenum in the environment. Residue Reviews. 1980; 74:1-43.

Jelikic-Stankova M, Uskokovic-Markovic S, Holclajtner-Antunovic I, Todorovic M, Djurdjevic P. Compounds of Mo, V and W in biochemistry and their biomed ical activity. J Trace Elem Med Biol. 2007; 21:8-16.

Ji C, Kaplowitz N, Lau MY, Kao E, Petrovic LM, Lee AS. Liver-specific loss of glucose-regulated protein 78 perturbs the unfolded protein response and exacerbates a spectrum of liver diseases in mice. Hepatology. 2011; 54:229-239.

Jiang S, Yan C, Fang QC, Shao ML, Zhang YL, Liu Y, Deng YP, Shan B, Liu JQ, Li HT, Yang L, Zhou J, Dai Z, Liu Y, Jia WP. Fibroblast growth factor 21 is regulated by the IRE1α-XBP1 branch of the unfolded protein response and

counteracts endoplasmic reticulum stress-induced hepatic steatosis. J Biol Chem. 2014; 289:29751-29765.

Johnson LJ. Molybdenum. In: O'Dell BL and Sunde RA., etds. Handbook of Nutritionally Essential Mineral Elements. Marcel Dekker. New York, 1997; 413-438.

Jung YA, Choi YK, Jung GS, Seo HY, Kim HS, Jang BK, Kim JG, Lee IK, Kim MK, Park KG. Sitagliptin attenuates methionine/choline-deficient diet-induced steatohepatitis. Diabetes Res Clin Pract. 2014; 105:47-57.

Kammoun HL, Chabanon H, Hainault I, Luquet S, Magnan C, Koike T, Ferré P, Foufelle F. GRP78 expression inhibits insulin and ER stress-induced SREBP-1c activation and reduces hepatic steatosis in mice. J Clin Invest. 2009; 119:1201-1215.

Karnikowski M, Córdova C, Oliveira RJ, Karnikowski MG, Nóbrega Ode T. Non-alcoholic fatty liver disease and metabolic syndrome in Brazilian middle-aged and older adults. Sao Paulo Med J. 2007; 125:333-337.

Khademi A, Azimirad R, Zavarian AA, and Moshfegh AZ.

Growth and Field Emission Study of Molybdenum Oxide Nanostars. J Phys Chem C. 2009; 113:19298-19304.

Kim SW, Hur W, Li TZ, Lee YK, Choi JE, Hong SW, Lyoo KS, You CR, Jung ES, Jung CK, Park T, Um SJ, Yoon SK. Oleuropein prevents the progression of steatohepatitis to hepatic fibrosis induced by a high-fat diet in mice. Exp Mol Med. 2014; 46:e92.

Kim S, Lee SH, Lee S, Park JD, Ryu DY. Arsenite-induced changes in hepatic protein abundance in cynomolgus monkeys (Macaca fascicularis). Proteomics. 2014; 14:1833-1843.

Kleiner DE, Brunt EM, Van Natta M, Behling C, Contos MJ, Cummings OW, Ferrell LD, Liu YC, Torbenson MS, Unalp-Arida A, Yeh M, McCullough AJ, Sanyal AJ; Nonalcoholic Steatohepatitis Clinical Research Network. Design and validation of a histological scoring system for nonalcoholic fatty liver disease. Hepatology. 2005; 41:1313-1321.

Komatsu M, Kurokawa H, Waguri S, Taguchi K, Kobayashi A, Ichimura Y, Sou YS, Ueno I, Sakamoto A, Tong KI, Kim M, Nishito Y, Iemura S, Natsume T, Ueno T, Kominami E,

Motohashi H, Tanaka K, Yamamoto M. The selective autophagy substrate p62 activates the stress responsive transcription factor Nrf2 through inactivation of Keap1. Nat Cell Biol. 2010; 12:213-223.

Komatsu M, Waguri S, Koike M, Sou YS, Ueno T, Hara T, Mizushima N, Iwata J, Ezaki J, Murata S, Hamazaki J, Nishito Y, Iemura S, Natsume T, Yanagawa T, Uwayama J, Warabi E, Yoshida H, Ishii T, Kobayashi A, Yamamoto M, Yue Z, Uchiyama Y, Kominami E, Tanaka K. Homeostatic levels of p62 control cytoplasmic inclusion body formation in autophagy deficient mice. Cell. 2007; 131:1149-1163.

Kovalskiy VV, Yarovaya GA, Shmavonyan DM. Changes of purine metabolism in man and animals under conditions of molybdenum biogeochemical provinces. Zh Obshch Biol. 1961; 22:179-191.

Krautbauer S, Eisinger K, Lupke M, Wanninger J, Ruemmele P, Hader Y, Weiss TS, Buechler C. Manganese superoxide dismutase is reduced in the liver of male but not female humans and rodents with non-alcoholic fatty liver disease. Exp Mol Pathol. 2013; 95:330-335.

Lake AD, Novak P, Hardwick RN, Flores-Keown B, Zhao F, Klimecki WT, Cherrington NJ. The adaptive endoplasmic reticulum stress response to lipotoxicity in progressive human nonalcoholic fatty liver disease. Toxicol Sci. 2014; 137:26-35.

Lamand M, Lab C, Tressol JC, Mason J. Biochemical parameters useful for the diagnosis of mild molybdenosis in sheep. Ann Rech Vet. 1980; 11:141-145.

Lavine JE, Schwimmer JB, Van Natta ML, Molleston JP, Murray KF, Rosenthal P, Abrams SH, Scheimann AO, Sanyal AJ, Chalasani N, Tonascia J, Ünalp A, Clark JM, Brunt EM, Kleiner DE, Hoofnagle JH, Robuck PR; Nonalcoholic Steatohepatitis Clinical Research Network. Effect of vitamin E or metformin for treatment of nonalcoholic fatty liver disease in children and adolescents: the TONIC randomized controlled trial. JAMA. 2011; 305:1659-1668.

Lazo M, Hernaez R, Eberhardt MS, Bonekamp S, Kamel I, Guallar E, Koteish A, Brancati FL, Clark JM. Prevalence of nonalcoholic fatty liver disease in the United States: the Third National Health and Nutrition Examination Survey, 1988-1994. Am J Epidemiol. 2013; 178:38-45.

Leclercq IA, Farrell GC, Schriemer R, Robertson GR. Leptin is essential for the hepatic fibrogenic response to chronic liver injury. J Hepatol. 2002; 37:206-213.

Lee HJ, Adham IM, Schwarz G, Kneussel M, Sass JO, Engel W, Reiss J. Molybdenum cofactor-deficient mice resemble the phenotype of human patients. Hum Mol Genet. 2002; 11:3309-3317.

Lee AH, Iwakoshi NN, Glimcher LH. XBP-1 regulates a subset of endoplasmic reticulum resident chaperone genes in the unfolded protein response. Mol Cell Biol. 2003; 23:7448-7459.

Lee S, Kim S, Hwang S, Cherrington NJ, Ryu DY. Dysregulated expression of proteins associated with ER stress, autophagy and apoptosis in tissues from nonalcoholic fatty liver disease. Oncotarget. 2017; 8:63370-63381.

Lewis RC, Johns LE, Meeker JD. Exploratory analysis of the potential relationship between urinary molybdenum and bone mineral density among adult men and women from NHANES 2007-2010. Chemosphere. 2016; 164:677-682.

Li J, Huang J, Li JS, Chen H, Huang K, Zheng L. Accumulation of endoplasmic reticulum stress and lipogenesis in the liver through generational effects of high fat diets. J Hepatol. 2012; 56:900-907.

Liangpunsakul S, Chalasani N. What should we recommend to our patients with NAFLD regarding alcohol use? Am J Gastroenterol. 2012; 107:976-978.

Listenberger LL, Han X, Lewis SE, Cases S, Farese RV Jr, Ory DS, Schaffer JE. Triglyceride accumulation protects against fatty acid-induced lipotoxicity. Proc Natl Acad Sci U S A. 2003; 100:3077-3082.

Lord SJ, Epstein NA, Paddock RL, Vogels CM, Hennigar TL, Zaworotko MJ, et al. Synthesis, characterization and biological relevance of hydroxypyrone and hydroxypyridinone complexes of molybdenum. Can J Chem. 1999; 77:1249-1261.

Loomba R, Lutchman G, Kleiner DE, Ricks M, Feld JJ, Borg BB, Modi A, Nagabhyru P, Sumner AE, Liang TJ, Hoofnagle JH. Clinical trial: pilot study of metformin for the treatment of non-alcoholic steatohepatitis. Aliment Pharmacol Ther. 2009;

29:172-182.

Ludwig J, Viggiano TR, McGill DB, Oh BJ. Nonalcoholic steatohepatitis: Mayo Clinic experiences with a hitherto unnamed disease. Mayo Clin Proc. 1980; 55:434-438.

Luo XM, Wei HJ, Yang SP. Inhibitory effects of molybdenum on esophageal and forestomach carcinogenesis in rats. J Natl Cancer Inst. 1983; 71: 75-80.

Määttänen P, Gehring K, Bergeron JJ, Thomas DY. Protein quality control in the ER: the recognition of misfolded proteins. Semin Cell Dev Biol. 2010; 21:500-511.

Machado MV, Michelotti GA, Xie G, Almeida Pereira T, Boursier J, Bohnic B, Guy CD, Diehl AM. Mouse models of diet-induced nonalcoholic steatohepatitis reproduce the heterogeneity of the human disease. PLoS One. 2015; 10:e0127991.

Malaguarnera L, Madeddu R, Palio E, Arena N, Malaguarnera M. Heme oxygenase-1 levels and oxidative stress-related parameters in non-alcoholic fatty liver disease patients. J

Hepatol. 2005; 42:585-591.

Mancinelli R, Ceccanti M. Biomarkers in alcohol misuse: their role in the prevention and detection of thiamine deficiency. Alcohol Alcohol. 2009; 44:177-182.

Marrero JA, Fontana RJ, Su GL, Conjeevaram HS, Emick DM, Lok AS. NAFLD may be a common underlying liver disease in patients with hepatocellular carcinoma in the United States. Hepatology. 2002; 36:1349-1354.

Matsumoto M, Hada N, Sakamaki Y, Uno A, Shiga T, Tanaka C, Ito T, Katsume A, Sudoh M. An improved mouse model that rapidly develops fibrosis in non-alcoholic steatohepatitis. Int J Exp Pathol. 2013; 94:93-103.

Matsunaga K, Saitoh T, Tabata K, Omori H, Satoh T, Kurotori N, Maejima I, Shirahama-Noda K, Ichimura T, Isobe T, Akira S, Noda T, Yoshimori T. Two Beclin 1-binding proteins, Atg14L and Rubicon, reciprocally regulate autophagy at different stages. Nat Cell Biol. 2009; 11:385-396.

McCullough KD, Martindale JL, Klotz LO, Aw TY, Holbrook

NJ. Gadd153 sensitizes cells to endoplasmic reticulum stress by down-regulating Bcl2 and perturbing the cellular redox state. Mol Cell Biol. 2001; 21:1249-1259.

Mizushima N, Levine B. Autophagy in mammalian development and differentiation. Nat Cell Biol. 2010; 12:823-830.

Meeker JD, Rossano MG, Protas B, Diamond MP, Puscheck E, Daly D, Paneth N, Wirth JJ. Cadmium, lead, and other metals in relation to semen quality: human evidence for molybdenum as a male reproductive toxicant. Environ Health Perspect. 2008; 116:1473-1479.

Meeker JD, Rossano MG, Protas B, Padmanahban V, Diamond MP, Puscheck E, Daly D, Paneth N, Wirth JJ. Environmental exposure to metals and male reproductive hormones: circulating testosterone is inversely associated with blood molybdenum. Fertil Steril. 2010; 93:130-140.

Mendel RR. Biology of the molybdenum cofactor. J Exp Bot. 2007; 58:2289-2296.

Mendel RR, Kruse T. Cell biology of molybdenum in plants and

humans. Biochim Biophys Acta. 2012; 1823:1568-1579.

Miao L, St Clair DK. Regulation of superoxide dismutase genes: implications in disease. Free Radic Biol Med. 2009; 47:344-356.

Momcilović B. A case report of acute human molybdenum toxicity from a dietary molybdenum supplement--a new member of the "Lucor metallicum" family. Arh Hig Rada Toksikol. 1999; 50:289-297.

Motomura W, Inoue M, Ohtake T, Takahashi N, Nagamine M, Tanno S, Kohgo Y, Okumura T. Up-regulation of ADRP in fatty liver in human and liver steatosis in mice fed with high fat diet. Biochem Biophys Res Commun. 2006; 340:1111-1118.

Mridha AR, Wree A, Robertson AAB, Yeh MM, Johnson CD, Van Rooyen DM, Haczeyni F, Teoh NC, Savard C, Ioannou GN, Masters SL, Schroder K, Cooper MA, Feldstein AE, Farrell GC. NLRP3 inflammasome blockade reduces liver inflammation and fibrosis in experimental NASH in mice. J Hepatol. 2017; 66:1037-1046.

Murray FJ, Sullivan FM, Tiwary AK, Carey S. 90-Day

subchronic toxicity study of sodium molybdate dihydrate in rats. Regul Toxicol Pharmacol. 2014; 70:579-588.

Mwangi SM, Peng S, Nezami BG, Thorn N, Farris AB 3rd, Jain S, Laroui H, Merlin D, Anania F, Srinivasan S. Glial cell line-derived neurotrophic factor protects against high-fat diet-induced hepatic steatosis by suppressing hepatic PPAR-γ expression. Am J Physiol Gastrointest Liver Physiol. 2016; 310:G103-G116.

Neuschwander-Tetri BA. Nonalcoholic steatohepatitis and the metabolic syndrome. Am J Med Sci. 2005; 330:326-335.

Neuschwander-Tetri BA. Hepatic lipotoxicity and the pathogenesis of nonalcoholic steatohepatitis: the central role of nontriglyceride fatty acid metabolites. Hepatology. 2010; 52:774-788.

Nouri M, Chalian H, Bahman A, Mollahajian H, Ahmadi-Faghih M, Fakheri H, Soroush A. Nail molybdenum and zinc contents in populations with low and moderate incidence of esophageal cancer. Arch Iran Med. 2008; 11:392-396.

Novotny JA, Turnlund JR. Molybdenum intake influences molybdenum kinetics in men. J Nutr. 2007; 137:37-42.

Oh SW, Han KH, Han SY. Associations between renal hyperfiltration and serum alkaline phosphatase. PLoS One. 2015; 10:e0122921.

Otomo C, Metlagel Z, Takaesu G, Otomo T. Structure of the human ATG12~ATG5 conjugate required for LC3 lipidation in autophagy. Nat Struct Mol Biol. 2013; 20:59-66.

Pagliassotti MJ. Endoplasmic reticulum stress in nonalcoholic fatty liver disease. Annu Rev Nutr. 2012; 32:17-33.

Pandey R, Singh SP. Effects of molybdenum on fertility of male rats. Biometals. 2002; 15:65-72.

Pankiv S, Clausen TH, Lamark T, Brech A, Bruun JA, Outzen H, Øvervatn A, Bjørkøy G, Johansen T. p62/SQSTM1 binds directly to Atg8/LC3 to facilitate degradation of ubiquitinated protein aggregates by autophagy. J Biol Chem. 2007; 282:24131-24145.

Panneerselvam SR, Govindasamy S. Sodium molybdate improves the phagocytic function in alloxan-induced diabetic rats. Chem Biol Interact. 2003; 145:159-163.

Panneerselvam SR, Govindasamy S. Effect of sodium molybdate on the status of lipids, lipid peroxidation and antioxidant systems in alloxan-induced diabetic rats. Clin Chim Acta. 2004; 345:93-98.

Poirier S, Mamarbachi M, Chen WT, Lee AS, Mayer G. GRP94 Regulates Circulating Cholesterol Levels through Blockade of PCSK9-Induced LDLR Degradation. Cell Rep. 2015; 13:2064-2071.

Puri P, Mirshahi F, Cheung O, Natarajan R, Maher JW, Kellum JM, Sanyal AJ. Activation and dysregulation of the unfolded protein response in nonalcoholic fatty liver disease. Gastroenterology. 2008; 134:568-576.

Puthalakath H, O'Reilly LA, Gunn P, Lee L, Kelly PN, Huntington ND, Hughes PD, Michalak EM, McKimm Breschkin J, Motoyama N, Gotoh T, Akira S, Bouillet P, Strasser A. ER stress triggers apoptosis by activating BH3-only protein Bim.

Cell. 2007; 129:1337-1349.

Raisbeck MF, Siemion RS, Smith MA. Modest copper supplementation blocks molybdenosis in cattle. J Vet Diagn Invest. 2006; 18:566-572.

Rajagopalan KV. Molybdenum: an essential trace element in human nutrition. Annu Rev Nutr. 1988; 8:401-427.

Rao A, Kosters A, Mells JE, Zhang W, Setchell KD, Amanso AM, Wynn GM, Xu T, Keller BT, Yin H, Banton S, Jones DP, Wu H, Dawson PA, Karpen SJ. Inhibition of ileal bile acid uptake protects against nonalcoholic fatty liver disease in high-fat diet-fed mice. Sci Transl Med. 2016; 8:357ra122.

Ratziu V, Harrison SA, Francque S, Bedossa P, Lehert P, Serfaty L, Romero-Gomez M, Boursier J, Abdelmalek M, Caldwell S, Drenth J, Anstee QM, Hum D, Hanf R, Roudot A, Megnien S, Staels B, Sanyal A; GOLDEN-505 Investigator Study Group. Elafibranor, an Agonist of the Peroxisome Proliferator-Activated Receptor-α and -δ, Induces Resolution of Nonalcoholic Steatohepatitis Without Fibrosis Worsening. Gastroenterology. 2016; 150:1147-1159.e5.

Ray SS, Das D, Ghosh T, Ghosh AK. The levels of zinc and molybdenum in hair and food grain in areas of high and low incidence of esophageal cancer: a comparative study. Glob J Health Sci. 2012; 4:168-175.

Redman BG, Esper P, Pan Q, Dunn RL, Hussain HK, Chenevert T, Brewer GJ, Merajver SD. Phase II trial of tetrathiomolybdate in patients with advanced kidney cancer. Clin Cancer Res. 2003; 9:1666-1672.

Reiss J, Bonin M, Schwegler H, Sass JO, Garattini E, Wagner S, Lee HJ, Engel W, Riess O, Schwarz G. The pathogenesis of molybdenum cofactor deficiency, its delay by maternal clearance, and its expression pattern in microarray analysis. Mol Genet Metab. 2005; 85:12-20.

Rinella ME, Elias MS, Smolak RR, Fu T, Borensztajn J, Green RM. Mechanisms of hepatic steatosis in mice fed a lipogenic methionine choline-deficient diet. J Lipid Res. 2008; 49:1068-1076.

Rinella ME, Green RM. The methionine choline deficient dietary model of steatohepatitis does not exhibit insulin

resistance. J Hepatol. 2004; 40:47-51.

Rinella ME, Siddiqui MS, Gardikiotes K, Gottstein J, Elias M, Green RM. Dysregulation of the unfolded protein response in db/db mice with diet-induced steatohepatitis. Hepatology. 2011; 54:1600-1609.

Rizki G, Arnaboldi L, Gabrielli B, Yan J, Lee GS, Ng RK, Turner SM, Badger TM, Pitas RE, Maher JJ. Mice fed a lipogenic methionine-choline-deficient diet develop hypermetabolism coincident with hepatic suppression of SCD-1. J Lipid Res. 2006; 47:2280-2290.

Ron D, Walter P. Signal integration in the endoplasmic reticulum unfolded protein response. Nat Rev Mol Cell Biol. 2007; 8:519-529.

Rutkevich LA, Williams DB. Participation of lectin chaperones and thiol oxidoreductases in protein folding within the endoplasmic reticulum. Curr Opin Cell Biol. 2011; 23:157-166.

Salmon DM, Flatt JP. Effect of dietary fat content on the incidence of obesity among ad libitum fed mice. Int J Obes.

1985; 9:443-449.

Sano R, Reed JC. ER stress-induced cell death mechanisms. Biochim Biophys Acta. 2013; 1833:3460-3470.

Sato K, Gosho M, Yamamoto T, Kobayashi Y, Ishii N, Ohashi T, Nakade Y, Ito K, Fukuzawa Y, Yoneda M. Vitamin E has a beneficial effect on nonalcoholic fatty liver disease: a meta-analysis of randomized controlled trials. Nutrition. 2015; 31:923-930.

Schumacker PT. Reactive oxygen species in cancer: a dance with the devil. Cancer Cell. 2015; 27:156-157.

Schuster S, Cabrera D, Arrese M, Feldstein AE. Triggering and resolution of inflammation in NASH. Nat Rev Gastroenterol Hepatol. 2018; 15:349-364.

Seki S, Kitada T, Yamada T, Sakaguchi H, Nakatani K, Wakasa K. In situ detection of lipid peroxidation and oxidative DNA damage in non-alcoholic fatty liver diseases. J Hepatol. 2002; 37:56-62.

Sevier CS, Kaiser CA. Ero1 and redox homeostasis in the endoplasmic reticulum. Biochim Biophys Acta. 2008; 1783:549-556.

Sha H, Yang L, Liu M, Xia S, Liu Y, Liu F, Kersten S, Qi L. Adipocyte spliced form of X-box-binding protein 1 promotes adiponectin multimerization and systemic glucose homeostasis. Diabetes. 2014; 63:867-879.

Shen L, Fan JG, Shao Y, Zeng MD, Wang JR, Luo GH, Li JQ, Chen SY. Prevalence of nonalcoholic fatty liver among administrative officers in Shanghai: an epidemiological survey. World J Gastroenterol. 2003; 9:1106-1110.

Singh R, Kaushik S, Wang Y, Xiang Y, Novak I, Komatsu M, Tanaka K, Cuervo AM, Czaja MJ. Autophagy regulates lipid metabolism. Nature. 2009; 458:1131-1135.

Skop V, Cahová M, Papáčková Z, Páleníčková E, Daňková H, Baranowski M, Zabielski P, Zdychová J, Zídková J, Kazdová L. Autophagy-lysosomal pathway is involved in lipid degradation in rat liver. Physiol Res. 2012; 61:287-297.

Sutti S, Jindal A, Locatelli I, Vacchiano M, Gigliotti L, Bozzola C, Albano E. Adaptive immune responses triggered by oxidative stress contribute to hepatic inflammation in NASH. Hepatology. 2014; 59:886-897.

Swenson TL, Casida JE. Aldehyde oxidase importance in vivo in xenobiotic metabolism: imidacloprid nitroreduction in mice. Toxicol Sci. 2013; 133:22-28.

Tabas I, Ron D. Integrating the mechanisms of apoptosis induced by endoplasmic reticulum stress. Nat Cell Biol. 2011; 13:184-190.

Tahan V, Canbakan B, Balci H, Dane F, Akin H, Can G, Hatemi I, Olgac V, Sonsuz A, Ozbay G, Yurdakul I, Senturk H. Serum gamma-glutamyltranspeptidase distinguishes non-alcoholic fatty liver disease at high risk. Hepatogastroenterology. 2008; 55:1433-1438.

Tanaka S, Hikita H, Tatsumi T, Sakamori R, Nozaki Y, Sakane S, Shiode Y, Nakabori T, Saito Y, Hiramatsu N, Tabata K, Kawabata T, Hamasaki M, Eguchi H, Nagano H, Yoshimori T, Takehara T. Rubicon inhibits autophagy and accelerates

hepatocyte apoptosis and lipid accumulation in nonalcoholic fatty liver disease in mice. Hepatology. 2016; 64:1994-2014.

Targher G, Bertolini L, Padovani R, Rodella S, Tessari R, Zenari L, Day C, Arcaro G. Prevalence of nonalcoholic fatty liver disease and its association with cardiovascular disease among type 2 diabetic patients. Diabetes Care. 2007; 30:1212-1218.

Tejada-Jiménez M, Galván A, Fernández E. Algae and humans share a molybdate transporter. Proc Natl Acad Sci U S A. 2011; 108:6420-6425.

Tejada-Jiménez M, Llamas A, Sanz-Luque E, Galván A, Fernández E. A high-affinity molybdate transporter in eukaryotes. Proc Natl Acad Sci U S A. 2007; 104:20126-20130.

Tewari M, Quan LT, O'Rourke K, Desnoyers S, Zeng Z, Beidler DR, Poirier GG, Salvesen GS, Dixit VM. Yama/CPP32 beta, a mammalian homolog of CED-3, is a CrmA-inhibitable protease that cleaves the death substrate poly (ADP-ribose) polymerase. Cell. 1995; 81:801-809.

Thompson KH, Chiles J, Yuen VG, Tse J, McNeill JH, Orvig C. Comparison of anti hyperglycemic effect amongst vanadium, molybdenum and other metal maltol complexes. J Inorg Biochem. 2004; 98:683-690.

Tilg H, Moschen AR. Evolution of inflammation in nonalcoholic fatty liver disease: the multiple parallel hits hypothesis. Hepatology. 2010; 52:1836-1846.

Trak-Smayra V, Paradis V, Massart J, Nasser S, Jebara V, Fromenty B. Pathology of the liver in obese and diabetic ob/ob and db/db mice fed a standard or high-calorie diet. Int J Exp Pathol. 2011; 92:413-421.

Tu QQ, Zheng RY, Li J, Hu L, Chang YX, Li L, Li MH, Wang RY, Huang DD, Wu MC, Hu HP, Chen L, Wang HY. Palmitic acid induces autophagy in hepatocytes via JNK2 activation. Acta Pharmacol Sin. 2014; 35:504-512.

Turnlund JR, Keyes WR, Peiffer GL. Molybdenum absorption, excretion, and retention studied with stable isotopes in young men at five intakes of dietary molybdenum. Am J Clin Nutr. 1995; 62:790-796.

van Galen P, Kreso A, Mbong N, Kent DG, Fitzmaurice T, Chambers JE, Xie S, Laurenti E, Hermans K, Eppert K, Marciniak SJ, Goodall JC, Green AR, Wouters BG, Wienholds E, Dick JE. The unfolded protein response governs integrity of the haematopoietic stem-cell pool during stress. Nature. 2014; 510:268-272.

Vyskocil A, Viau C. Assessment of molybdenum toxicity in humans. J Appl Toxicol. 1999; 19:185-192.

Walravens PA, Moure-Eraso R, Solomons CC, Chapell WR, Bentley G, Biochemical abnormalities in workers exposed to molybdenum dust. Arch Environ Health. 1979; 34:302-308.

Wang S, Chen Z, Lam V, Han J, Hassler J, Finck BN, Davidson NO, Kaufman RJ. IRE1α-XBP1s induces PDI expression to increase MTP activity for hepatic VLDL assembly and lipid homeostasis. Cell Metab. 2012; 16:473-486.

Wei HJ, Luo XM, Yang SP. Effects of molybdenum and tungsten on mammary carcinogenesis in SD rats. J Natl Cancer Inst. 1985; 74:469-473.

Weiß J, Rau M, Geier A. Non-alcoholic fatty liver disease: epidemiology, clinical course, investigation, and treatment. Dtsch Arztebl Int. 2014; 111:447-452.

Weston SR, Leyden W, Murphy R, Bass NM, Bell BP, Manos MM, Terrault NA. Racial and ethnic distribution of nonalcoholic fatty liver in persons with newly diagnosed chronic liver disease. Hepatology. 2005; 41:372-379.

Williams CD, Stengel J, Asike MI, Torres DM, Shaw J, Contreras M, Landt CL, Harrison SA. Prevalence of nonalcoholic fatty liver disease and nonalcoholic steatohepatitis among a largely middle-aged population utilizing ultrasound and liver biopsy: a prospective study. Gastroenterology. 2011; 140:124-131.

Williamson RM, Price JF, Glancy S, Perry E, Nee LD, Hayes PC, Frier BM, Van Look LA, Johnston GI, Reynolds RM, Strachan MW; Edinburgh Type 2 Diabetes Study Investigators. Prevalence of and risk factors for hepatic steatosis and nonalcoholic Fatty liver disease in people with type 2 diabetes: the Edinburgh Type 2 Diabetes Study. Diabetes Care. 2011; 34:1139-1144.

Wilson S, Chalasani N. Noninvasive markers of advanced histology in nonalcoholic fatty liver disease: are we there yet? Gastroenterology. 2007; 133:1377-1378.

Wong VW, Chu WC, Wong GL, Chan RS, Chim AM, Ong A, Yeung DK, Yiu KK, Chu SH, Woo J, Chan FK, Chan HL. Prevalence of non-alcoholic fatty liver disease and advanced fibrosis in Hong Kong Chinese: a population study using proton-magnetic resonance spectroscopy and transient elastography. Gut. 2012; 61:409-415.

Xiao SJ, Fu GJ, Lv YL, Zhong XN, Wang RH. Prevalence and risk factors of fatty liver disease in young and middle-aged population: one center study in Southwestern China. J Gastroenterol Hepatol. 2014; 29:358-364.

Xiao W, Ren M, Zhang C, Li S, An W. Amelioration of nonalcoholic fatty liver disease by hepatic stimulator substance via preservation of carnitine palmitoyl transferase-1 activity. Am J Physiol Cell Physiol. 2015; 309:C215-C227.

Yamagishi N, Ueda T, Mori A, Saito Y, Hatayama T. Decreased expression of endoplasmic reticulum chaperone

GRP78 in liver of diabetic mice. Biochem Biophys Res Commun. 2012; 417:364-370.

Yamaguchi H, Wang HG. CHOP is involved in endoplasmic reticulum stress-induced apoptosis by enhancing DR5 expression in human carcinoma cells. J Biol Chem. 2004; 279:45495-45502.

Yamane Y, Koizumi T. Protective effect of molybdenum on the acute toxicity of mercuric chloride. Toxicol Appl Pharmacol. 1982; 65:214-221.

Yamane Y, Fukuchi M, Chiko L, Koizumi T. Protective effect of sodium molybdate against the acute toxicity of cadmium chloride. Toxicology. 1990; 60:235-243.

Yoshida M. Novel role of NPC1L1 in the regulation of hepatic metabolism: potential contribution of ezetimibe in NAFLD/NASH treatment. Curr Vasc Pharmacol. 2011; 9:121-123.

Yoshida H, Haze K, Yanagi H, Yura T, Mori K. Identification of the cis-acting endoplasmic reticulum stress response element responsible for transcriptional induction of mammalian glucose-regulated proteins. Involvement of basic leucine zipper

transcription factors. J Biol Chem. 1998; 273:33741-33749.

Yoshida M, Nakagawa M, Hosomi R, Nishiyama T, Fukunaga K. Low molybdenum state induced by tungsten as a model of molybdenum deficiency in rats. Biol Trace Elem Res. 2015; 165:75-80.

Youle RJ, Strasser A. The BCL-2 protein family: opposing activities that mediate cell death. Nat Rev Mol Cell Biol. 2008; 9:47-59.

Youn P, Kim S, Ahn JH, Kim Y, Park JD, Ryu DY. Regulation of iron metabolism-related genes in diethylnitrosamine-induced mouse liver tumors. Toxicol Lett. 2009; 184:151-158.

Younossi ZM, Koenig AB, Abdelatif D, Fazel Y, Henry L, Wymer M. Global epidemiology of nonalcoholic fatty liver disease-Meta-analytic assessment of prevalence, incidence, and outcomes. Hepatology. 2016; 64:73-84.

Younossi ZM, Otgonsuren M, Henry L, Venkatesan C, Mishra A, Erario M, Hunt S. Association of nonalcoholic fatty liver disease (NAFLD) with hepatocellular carcinoma (HCC) in the

United States from 2004 to 2009. Hepatology. 2015; 62:1723-1730.

Zein CO, Yerian LM, Gogate P, Lopez R, Kirwan JP, Feldstein AE, McCullough AJ. Pentoxifylline improves nonalcoholic steatohepatitis: a randomized placebo-controlled trial. Hepatology. 2011; 54:1610-1619.

Zelber-Sagi S, Nitzan-Kaluski D, Halpern Z, Oren R. Prevalence of primary non-alcoholic fatty liver disease in a population-based study and its association with biochemical and anthropometric measures. Liver Int. 2006; 26:856-863.

Zhang X, Han J, Man K, Li X, Du J, Chu ES, Go MY, Sung JJ, Yu J. CXC chemokine receptor 3 promotes steatohepatitis in mice through mediating inflammatory cytokines, macrophages and autophagy. J Hepatol. 2016; 64:160-170.

Zhou WG, He LZ, Lin WY, Luo JH. Trace element measurement in gastric mucosa of gastric disease patients. Guangxi Med. 1990; 12:298-300.

Zhou H, Liu R. ER stress and hepatic lipid metabolism. Front

Genet. 2014; 5:112.

Zhu L, Baker SS, Liu W, Tao MH, Patel R, Nowak NJ, Baker RD. Lipid in the livers of adolescents with nonalcoholic steatohepatitis: combined effects of pathways on steatosis. Metabolism. 2011; 60:1001-1011.

Zinszner H, Kuroda M, Wang X, Batchvarova N, Lightfoot RT, Remotti H, Stevens JL, Ron D. CHOP is implicated in programmed cell death in response to impaired function of the endoplasmic reticulum. Genes Dev. 1998; 12: 982-995.

국문초록

비알콜성 지방간 질환에 대한 몰리브덴산염의 예방적 효과

이승우

서울대학교 대학원

수의병인생물학 및 예방수의학 (환경위생학) 전공

비알콜성 지방간 질환 (non-alcoholic fatty liver disease, NAFLD)은 단순 지방간 (non-alcoholic fatty liver, NAFL)과 지방간염 (non-alcoholic steatohepatitis, NASH)을 포함하는 질환으로 간경화 (cirrhosis) 및 간세포 암종 (hepatocellular carcinoma)을 포함한 말기 간 질환으로 진행될 수 있기 때문에 중요한 공중보건 문제로 다루어지고 있다. 그러나 NAFLD의 발병 기전은 완전히 규명되지 않았으며, 현재까지 치료제로서 미국 연방식품의약국의 승인을 받은 약물은 없다.

간 내 과도한 지방 축적은 NAFLD의 특징적인 병리학적

소견이며, 활성산소종 (reactive oxygen species)의 증가로 인한 산화적 스트레스 (oxidative stress)는 NAFLD 발병의 주요 인자로 알려져 있다. 그리고 NAFLD의 발병과 진행에 소포체 (endoplasmic reticulum, ER) 내 미접힘 단백질 (unfolded protein)의 축적에 의해 유발되는 소포체 스트레스 (ER stress)가 중요한 요소로 작용할 수 있다고 최근 보고되었다. 또한, 세포 내 손상된 소기관과 단백질, 지질 등을 분해하는 자가포식 (autophagy)작용이 NAFLD 발병과 관련이 있음을 시사하는 연구도 보고된 바 있다. Autophagy와 세포사멸 (apoptosis) 작용은 서로 억제하면서 교차 조절한다고 알려져 있다.

본 연구에서는 NAFLD의 분자생물학적 경로를 규명하고자 사람의 NASH, NAFL 그리고 정상 간 (normal) 조직에서 ER stress, apoptosis, autophagy와 관련된 단백질들의 발현 수준을 western blot을 통해 분석하였다. 그 결과, ER stress 신호전달 전사인자인 cleaved activating transcription factor 6 (ATF6), spliced X-box binding protein 1 (XBP1s) 그리고 CCAAT/enhancer binding protein (C/EBP) homologous protein (CHOP)의 단백질 발현 수준은 normal 조직에 비해 NASH 조직에서 더 높았다. 반면, 미접힘 단백질 반응 (unfolded protein response, UPR)에 관여하는 glucose-regulated protein 78 (GRP78)과 protein disulfide isomerase (PDI)를 포함한 ER 샤페론 및 폴딩 효소들의 발현 수준은 normal 조직에 비해 NASH 조직에서 더 낮았다. NASH 조직에서 B-cell lymphoma-2 (Bcl-2)

계열 단백질들의 발현 조절장애 (dysregulation)가 관찰된 가운데, cleaved poly (ADP-ribose) polymerase (PARP)과 같은 apoptosis 마커 단백질들의 발현 수준은 normal 조직에 비해 NASH 조직에서 더 낮았다. Autophagy 조절 인자인 autophagy protein 16L1 (ATG16L1)과 microtubule-associated proteins 1A/1B light chain 3-II (LC3-II)의 발현 수준은 normal 조직에 비해 NASH조직에서 더 높았지만, autophagy 기질 단백질인 p62은 두 조직 간에 유의한 발현 변화가 관찰되지 않았다. 위 3개 분자생물학적 경로와 관련된 단백질들의 NAFL 조직 내 발현은 normal 조직 또는 NASH 조직과 유사한 경향을 보이거나, 두 조직의 중간 수준이었다. 이러한 결과는 사람의 NAFLD 조직에서 UPR 및 apoptosis와 관련된 특정 중요 조직 과정의 조절이 광범위하게 손상되었음을 시사한다.

이전 연구에서 몰리브덴산염 (molybdate) 투여는 당뇨병 쥐의 지질 수준을 감소시키는 것으로 보고하였다. 또한, 산화방지제 (antioxidant)로서의 molybdate의 잠재적인 활성은 다양한 동물 모델에서도 입증되었다. 따라서, 본 연구에서는 광범위하게 사용되고 있는 대사성 질환 마우스 모델 중 하나인 메티오닌-콜린 결핍 식이 (methionine- and choline-deficient diet, MCD) 모델을 이용하여 NAFL 및 그와 관련된 장애에 대한 molybdate의 영향을 평가하였다. 10 주령의 수컷 C57BL/6 마우스에 MCD와 molybdate을 함유한 식수를 4 주간 투여하였다. 그 결과, molybdate 투여는 MCD에 의해 유발된 간 내 지질

축적을 현저히 약화시켰다. 그리고 MCD를 섭취한 마우스의 간에서 molybdate 투여는 LC3-II의 형성을 증가시킴과 동시에 p62 단백질의 발현 수준을 감소시킴으로서 지질 이화 작용과 관련된 autophagy 경로를 활성화시켰다. MCD에 의한 지질 및 단백질 산화와 같은 산화적 손상 (oxidative damage)도 간에서 molybdate에 의해 완화되었다. 반면, molybdate 투여는 MCD를 섭취한 마우스의 간에서 ER stress와 관련된 단백질들의 발현에는 영향을 미치지 않았다. 또한, MCD에 의한 간세포 손상 정도도 molybdate 투여에 의해 영향을 받지 않았다. 이러한 결과는 molybdate이 마우스 간에서 부작용을 일으키지 않으면서 MCD에 의해 유발된 NAFL을 autophagy 작용의 활성화를 통해 효과적으로 완화시킬 수 있음을 시사한다.

본 연구는 사람 NAFLD의 발병 기전에 대한 새로운 지견과 더불어 NAFLD의 치료 예방제로서 molybdate의 가능성을 제시하고 있다.

주요어: 비알콜성 지방간 질환, 몰리브덴산염, 소포체 스트레스, 산화적 스트레스, 자가포식, 세포사멸
학번: 2012-21546